

RESEARCH ARTICLE

Distribution of aromatase in the brain of the African cichlid fish *Astatotilapia burtoni*: Aromatase expression, but not estrogen receptors, varies with female reproductive-state

Karen P. Maruska¹  | Julie M. Butler¹  | Chase Anselmo¹ | Ganga Tandukar^{1,2}

¹Department of Biological Sciences, Louisiana State University, Baton Rouge, Louisiana

²Biology Program, University of Louisiana at Monroe, Monroe, Louisiana

Correspondence

Karen P. Maruska, Department of Biological Sciences, 202 Life Sciences Bldg., Louisiana State University, Baton Rouge, LA 70803.
Email: kmaruska@lsu.edu

Funding information

Louisiana Biomedical Research Network, Grant/Award Number: NIH P20 GM103424-17; Louisiana Board of Regents Fellowship; National Science Foundation Graduate Research Fellowship, Grant/Award Number: 1247192; National Science Foundation, Grant/Award Numbers: IOS-1456558, IOS-1456004

Peer Review

The peer review history for this article is available at <https://publons.com/publon/10.1002/cne.24908>.

Abstract

Estrogen synthesis and signaling in the brains of vertebrates has pleotropic effects ranging from neurogenesis to modulation of behaviors. The majority of studies on brain-derived estrogens focus on males, but estrogenic signaling in females likely plays important roles in regulation of reproductive cycling and social behaviors. We used females of the mouth brooding African cichlid fish, *Astatotilapia burtoni*, to test for reproductive state-dependent changes in estrogenic signaling capacity within microdissected brain nuclei that are important for social behaviors. Expression levels of the rate-limiting enzyme aromatase, but not estrogen receptors, measured by qPCR changes across the reproductive cycle. Gravid females that are close to spawning had higher aromatase levels in all brain regions compared to females with lower reproductive potential. This brain aromatase expression was positively correlated with circulating estradiol levels and ovarian readiness. Using chromogenic in situ hybridization we localized aromatase-expressing cells to ependymal regions bordering the ventricles from the forebrain to the hindbrain, and observed more abundant staining in gravid compared to mouth brooding females in most regions. Staining was most prominent in subpallial telencephalic regions, and diencephalic regions of the preoptic area, thalamus, and hypothalamus, but was also observed in sensory and sensorimotor areas of the midbrain and hindbrain. Aromatase expression was observed in radial glial cells, revealed by co-localization with the glial marker

Abbreviations: 4v, fourth ventricle; ac, anterior commissure; aGn, anterior glomerular nucleus; ATn, anterior tuberal nucleus; CC, cerebellar crest; CCeG,M,P, granular, molecular, and Purkinje layer of corpus cerebellum; Ce, cerebellum; CG, central gray; CM, corpus mammillare; CP, central posterior thalamic nucleus; CZ, central zone of tectum; Dc-1-4, central part of the dorsal telencephalon, subdivisions 1-4; Dd-v,-d, dorsal part of the dorsal telencephalon, ventral and dorsal subdivisions; Dl-d, dorsal part of the lateral part of the dorsal telencephalon; Dl-g, granular zone of the lateral part of the dorsal telencephalon; Dl-v1,-v2, ventral zone of the lateral part of the dorsal telencephalon, subdivisions 1, 2; Dm-1,-2r,-3, medial part of the dorsal telencephalon, subdivisions 1, 2 (rostral), and 3; DON, descending octaval nucleus; Dp, posterior part of the dorsal telencephalon; DP, dorsal posterior thalamic nucleus; DWZ, deep white zone of tectum; E, entopeduncular nucleus; GL, glomerular cell layer of olfactory bulb; Gn, glomerular nucleus; hc, horizontal commissure; Hyp, hypothalamus; Illn, oculomotor nucleus; ICL, internal cell layer of olfactory bulb; IP, interpeduncular nucleus; LFB, lateral forebrain bundle; LT, lateral thalamic nucleus; Med, medulla; MON, medial octavolateralis column; NC, nucleus corticalis; NDILc,l, central and lateral part of the diffuse nucleus of the inferior lobe; nHd,v, dorsal and ventral habenular nucleus; NLTd,i,m,v, lateral tuberal nucleus, dorsal, intermediate, medial, and ventral parts; nMLF, nucleus of medial longitudinal fasciculus; NP, paracommissural nucleus; nPPa, parvocellular preoptic nucleus, anterior part; nMMp, magnocellular preoptic nucleus, magnocellular division; nPMp, magnocellular preoptic nucleus, parvocellular division; nPPp, parvocellular preoptic nucleus, posterior part; NRL, nucleus of the lateral recess; NRP, nucleus of the posterior recess; NT, nucleus taenia; OC, optic chiasm; ON, optic nerve; PAG, periaqueductal gray; pc, posterior commissure; PGa,c,l,m, anterior, commissural, lateral, and medial pregglomerular nucleus; PGZ, periventricular gray zone of tectum; Pit, pituitary gland; POA, preoptic area; PSi,m, superficial pretectal nucleus, intermediate and medial subdivision; PSP, parvocellular superficial pretectal nucleus; PVO, paraventricular organ; Ri,s, inferior and superior reticular nucleus; SGn, secondary gustatory nucleus; sgt, secondary gustatory tract; smn, spinal motor neurons; SR, superior raphe nucleus; SWGZ, superficial gray and white zone of tectum; T, tectum; Tel, telencephalon; TGN, tertiary gustatory nucleus; TS, torus semicircularis; TSc, central nucleus of torus semicircularis; TSvl, ventrolateral nucleus of torus semicircularis; TL, torus longitudinalis; TLa, nucleus of the torus lateralis; TPp, periventricular nucleus of the posterior tuberculum; VAO, ventral accessory optic nucleus; Vc, central part of the ventral telencephalon; VCeG, granular layer of valvular cerebellum; Vd-c,-r, dorsal part of the ventral telencephalon, caudal and rostral subdivisions; Vde, descending tract of the trigeminal nerve; Vils, facial sensory nucleus; VI, lateral part of the ventral telencephalon; VL, vagal lobe; VMn, ventromedial thalamic nucleus; VOT, ventral optic tract; Vp, postcommissural nucleus of the ventral telencephalon; Vs-l,-m, lateral and medial part of the supracommissural nucleus of the ventral telencephalon; Vv, ventral part of the ventral telencephalon; Xm, vagal motor nucleus.

GFAP and absence of co-localization with the neuronal marker HuC/D. Collectively these results support the idea that brain-derived estradiol in females may serve important functions in reproductive state-dependent physiological and behavioral processes across vertebrates.

KEYWORDS

cyp19a1b, estradiol, neuroestrogen, RRID: AB_221448, RRID: AB_561049, RRID: AB_561049, RRID: SCR_003070, RRID: SCR_014199, RRID: SCR_014329, social behavior, steroid, teleost

1 | INTRODUCTION

Estrogens exert pleiotropic effects on both reproductive and non-reproductive functions in vertebrates, including modulation of behaviors. The enzyme aromatase catalyzes the conversion of testosterone to estrogens, which then bind to nuclear and membrane-bound estrogen receptors (estrogen receptors α and β ; G-protein coupled receptor 30, GPR30, also known as GPER) expressed in various target tissues to exert genomic and more rapid nongenomic effects. The gonads (ovary and testis) are a major source of circulating estrogens, but the brain also possesses all of the enzymatic players, including aromatase, to synthesize its own estrogens (i.e., neurosteroids) and expresses both nuclear and membrane-bound receptors in regions mediating behaviors, sensorimotor integration, and neuroendocrine function (Cornil & de Bournonville, 2018; Diotel et al., 2011; Forlano, Schlinger, & Bass, 2006; Shaw, 2018; Ubuka & Tsutsui, 2014; Vajaria & Vasudevan, 2018). In addition to regulating processes directly associated with reproduction, estrogen signaling in the brain is also involved in modulation of social communication circuits (Shaw, 2018), learning and memory (Luine, Serrano, & Frankfurt, 2018), and neuroplasticity, neurogenesis, and neuroprotection (Lai, Yu, Zhang, & Chen, 2017; Ponti, Farinetti, Marraudino, Panzica, & Gotti, 2018; Sheppard, Choleris, & Galea, 2019). Thus, estrogen signaling within neural circuits has the potential to influence an animal's biology and behavior at multiple levels.

The production of estrogens in the brain has important activational effects on adult social behaviors, physiology, and sensory processing associated with aggression, reproduction, and parental care across taxa. These estrogenic effects are primarily studied in males where many behavioral outcomes are due to aromatization of circulating androgens to estrogens (Cornil & de Bournonville, 2018). For example, estradiol facilitates paternal behavior in dwarf hamsters (Romero-Morales et al., 2018), increases male aggression in fishes, birds, and mammals (Huffman, O'Connell, & Hofmann, 2013; Schlinger & Callard, 1989; Trainor, Finy, & Nelson, 2008), and stimulates sexual behaviors such as mounting and copulation in castrated rodents and quail (Cornil, Dalla, Papadopoulou-Daifoti, Baillien, & Balthazart, 2006; Cross & Roselli, 1999). In contrast, since many female vertebrates typically have higher circulating estrogens compared to males, fewer studies focus on the potential roles of brain-produced estrogens in females. There is evidence, however, that

estrogens produced in the female brain could act either together with or independently from ovarian-derived estrogens (Cornil, 2018). In light of the numerous sex differences seen in brain and neural circuit function in all vertebrate groups, examining estrogen signaling pathways specifically in females, and comparing them to males of the same species, is important. Further, given the conserved expression of aromatase and estrogen receptors in nuclei of the social behavior network (Goodson, 2005; Newman, 1999) and social communication circuits (Shaw, 2018), central estrogen signaling likely plays an important but under-studied role in female social behaviors and reproductive cycling.

To study the importance of estrogen signaling in the brain of female vertebrates, it is useful to examine species with high levels of estrogen production and well-described social behaviors. Teleost fishes are ideal subjects because they typically have higher aromatase activity in the brain than in the gonads (G. V. Callard, Tchoudakova, Kishida, & Wood, 2001; Gonzalez & Piferrer, 2003), and have the highest levels of brain aromatase of any vertebrate ($\times 100$ –1,000 greater activity in the preoptic area-hypothalamus than in mammals; G. Callard, Schlinger, & Pasmanik, 1990; Pasmanik & Callard, 1985). Most teleost fishes have two aromatase genes, *cyp19a1a* (gonadal) and *cyp19a1b* (brain), which also contain an estrogen-responsive element (ERE) in the promoter region so that its activity is stimulated by estrogen itself in a positive autoregulatory loop (Diotel et al., 2010). Brain aromatase is abundant along ventricular surfaces in fishes, and primarily expressed in radial glial cells rather than in neurons as seen in birds and mammals (Balthazart et al., 2006; Forlano et al., 2006; Forlano, Deitcher, Myers, & Bass, 2001). Further, aromatase and estrogen receptors in the female brain are implicated in the control of ovarian readiness, as well as reproductive motivation and expression of behaviors (Diotel et al., 2010; Kayo, Zempo, Tomihara, Oka, & Kanda, 2019). Teleosts also display remarkable sexual plasticity throughout their lifetime, including sex-steroid modulation of sex-specific social behaviors after sexual maturity, making them excellent models to investigate neural mechanisms of activational hormone-modulated biological processes.

The African cichlid fish *Astatotilapia burtoni* (Gunther, 1894) in particular has emerged as a valuable neuroethological model for studying neural mechanisms underlying complex social behaviors (K. P. Maruska & Fernald, 2018). Females become gravid (ripe with eggs) and ovulate prior to showing affiliative behaviors and choosing a

male for spawning. During courtship and mate choice, females integrate salient information from visual (behavior and coloration changes), acoustic, chemosensory, mechanosensory, and tactile signals produced by dominant males (Butler et al., 2019; Field & Maruska, 2017; K. P. Maruska & Fernald, 2012; K. P. Maruska, Ung, & Fernald, 2012; K.P. Maruska & Fernald, 2014). Gravid and ovulated females also have improved hearing and vision compared to non-reproductive females, which may in part be mediated by estrogens (Butler et al., 2019; K. P. Maruska, Ung, et al, 2012). Postspawning females then carry the fertilized eggs and developing embryos in their mouths for ~2 weeks (mouth brooding), followed by fry release and a recovering period characterized by feeding and ovarian growth to prepare for subsequent spawning. Thus, each stage of the female reproductive cycle involves distinct behaviors, physiology, and sensory processing capabilities, which could be modulated by variations in estrogen signaling within localized neural circuits across the reproductive cycle. To our knowledge, no other study examined variations in aromatase and estrogenic signaling in a mouth brooding fish that deals with trade-offs between feeding/energetics, reproduction, and parental care.

The goals of this study were twofold. First, we tested for reproductive-state plasticity in estrogen signaling by measuring expression levels via qPCR of estrogen receptors and aromatase in microdissected nuclei of the female brain that are involved in social behaviors. Most previous studies across taxa examine changes in receptor and aromatase expression in either whole brain or large macrodissected brain regions (e.g., preoptic area-hypothalamus), but more localized changes in steroid sensitivity within a neural circuit could influence behavior, sensory processing, or other physiological processes on short and long time-scales (Balthazart, Taziaux, Holloway, Ball, & Cornil, 2009; Ramage-Healey & Bass, 2006; Ramage-Healey, Maidment, & Schlinger, 2008). Second, because local estrogen production in the brain may have important roles in mediating reproductive-cycle related estrogen availability, we also mapped the distribution of aromatase-expressing cells in the cichlid brain. While aromatase is localized and mapped in the brain of several other fishes (see Table 1), no study examined brain aromatase in a maternal mouth brooding fish with nonseasonal cycling. Determining reproductive-specific brain expression of aromatase in different species can be informative for identifying behavioral circuits that might be influenced by estrogen signaling, or are under local control by estrogen, particularly in a comparative and evolutionary context.

2 | MATERIALS AND METHODS

2.1 | Animals and tissue collection

African cichlid fish *A. burtoni* (Gunther, 1894) were from an originally derived population collected from Lake Tanganyika, Africa, in the 1970's and subsequently bred in the laboratory. Fish were maintained in mixed-sex groups in flow-through 30 L aquaria under conditions similar to what they experience in the African lake (pH 8.0, 28–30°C,

300–50 $\mu\text{S cm}^{-1}$, 12 L:12D light cycle, constant aeration). Fish were fed cichlid flakes daily (Aquadine, Healdsburg, CA) and supplemented with brine shrimp several times a week. All experiments were performed in accordance with the recommendations and guidelines provided by the National Institutes of Health Guide for the Care and Use of Laboratory Animals, 2011. The protocol was approved by the Institutional Animal Care and Use Committee (IACUC) at Louisiana State University, Baton Rouge, LA.

The female *A. burtoni* reproductive cycle includes a period of ovarian recrudescence when oocytes enlarge and undergo vitellogenesis as the female becomes gravid. After ovulation, a female will spawn with one or more males by depositing eggs on the substrate, immediately picking them up into her mouth, and then nipping at the dominant male's anal fin egg spots to initiate sperm release and fertilization of the eggs in her mouth. Females then brood the developing young inside their mouths for ~2 weeks before releasing them as free-swimming fry. After mouth brooding and maternal care, females go through a recovering period to prepare for subsequent spawning cycles. We collected gravid, recovering, and mouth brooding females from mixed-sex community tanks in the morning (08:00–09:30 am) prior to feeding. Gravid females were selected based on distended abdomens characteristic of large ova, and later verified to have gonadosomatic index (GSI) values ≥ 7.0 . Mouth brooding females were sampled mid-way through the brood cycle (day 6–8) and had GSI values ≤ 1.5 . Recovering females were fish between brooding and gravid states with GSI values of 1.5–4.0. Fish were quickly netted from aquaria and measured for standard length (SL) and body mass (BM). Brooding, recovering, and gravid females all had similar standard lengths (one-way ANOVA, $F_{2,33} = 2.58$, $p = .091$), but gravid females had greater body mass (one-way ANOVA, $F_{2,33} = 7.49$, $p = .002$) compared to both brooding (SNK, $p = .003$) and recovering (SNK, $p = .004$) females. This is likely due to the large ova in gravid females. Blood was collected from the caudal vein with heparinized capillary tubes, centrifuged for 10 min at 8000 rpm, and plasma removed and stored at -80°C until assayed. Fish were immobilized in ice-cold water, sacrificed by rapid cervical transection, and brains were removed and embedded in OCT mounting media on dry ice followed by storage at -80°C until sectioning. Ovaries were removed and weighed to calculate gonadosomatic index [GSI = (ovary mass/BM) \times 100].

2.2 | Steroid hormone assays

Circulating plasma levels of 17β -estradiol (E2) and 11-ketotestosterone (11KT) were measured using enzyme immunoassay kits (Cayman Chemical Company, Ann Arbor, MI.: Estradiol #582252, 11KT #582751) as previously described and validated in *A. burtoni* (K. P. Maruska, 2015; K. P. Maruska & Fernald, 2010b). While we did not measure the aromatizable testosterone (T) in this study because of limited available plasma, previous work in *A. burtoni* showed that plasma T levels are highly correlated with 11KT and E2, and differ among female reproductive states in a similar manner to that observed here for E2

TABLE 1 Comparative distribution of aromatase expression (AROMB, *aromb*, *cyp19a1b*) determined by immunohistochemistry or in situ hybridization in the brain of teleosts

	<i>Astatotilapia burtoni</i> (African cichlid) ^a	<i>Porichthys notatus</i> (midshipman) ^b	<i>Danio rerio</i> (zebrafish) ^c	<i>Odontesthes bonariensis</i> (pejerrey) ^d	<i>Oncorhynchus mykiss</i> (rainbow trout) ^e	<i>Thalassoma bifasciatum</i> (bluehead wrasse) ^f	<i>Apteronotus leptorhynchus</i> (brown ghost knifefish) ^g	<i>Oryzias latipes</i> (medaka) ^h	<i>Anguilla japonica</i> (Japanese eel) ^{i,j}
Forebrain									
Olfactory bulbs	+	+	+	Nd	+	Nd	-	+	-
Ventral telencephalon (subpallial regions)	+	+	+	+	+	+	+	+	+
Dorsal telencephalon (pallial regions)	+	+	+	+	+	+	+	+	+
Preoptic area	+	+	+	+	+	+	+	+	+
Thalamus	+	+	+	Nd	+	+	-	+	+
Habenula	+	Nd	+	Nd	Nd	+	+	+	Nd
Hypothalamus (lateral recess)	+	+	+	Nd	+	+	+	+	+
Hypothalamus (inferior lobe)	-	+	+	Nd	Nd	+	-	-	Nd
Ventral hypothalamus (tuberal regions)	+	+	+	+	+	+	+	+	+
Pituitary	+	+	+	+	+	Nd	+	+	+
Midbrain									
Tectum	+	-	+	+	+	+	-	+(f)	Nd
Torus semicircularis	+	-	+	+	+	+	-	+	Nd
Hindbrain									
Cerebellum	+	-	+	Nd	-	+	-	+	-
Medulla	+	+	+	Nd	+	+	-	Nd	-

Note: +, present; -(f), present in females only; -, absent; nd, not determined.

^aThis study.

^bForlano et al. (2001).

^cGoto-Kazeto, Kight, Zohar, Place, and Trant (2004).

^dStrobl-Mazzulla et al. (2005, 2008).

^eMenuet et al. (2003).

^fMarsh, Creutz, Hawkins, and Godwin (2006).

^gShaw and Krahe (2018) and Shaw (2018).

^hOkubo et al. (2011).

ⁱJeng et al. (2012).

^jJapanese eel have only one aromatase gene, *cyp19a1*, which shows similar distribution to *cyp19a1b* in other teleosts.

and 11KT levels (gravid > recovering > brooding) (K. P. Maruska & Fernald, 2010a, 2010b). Serum samples were extracted three times with 200 μ l of diethyl ether, evaporated in a fume hood at room temperature, and reconstituted in kit assay buffer (1:35 dilution). Each sample was assayed in duplicate for each hormone, kit protocols were strictly followed, and each plate was read in triplicate at 405 nm. Concentrations were determined based on standard curves, and intra-assay coefficients of variation (CV) were 10.1% (E2) and 9.5% (11KT).

2.3 | Microdissection, RNA isolation, and quantitative reverse transcription PCR

To examine genes involved in estrogen signaling (aromatase, estrogen receptors) within localized regions of the female brain, brains were sectioned in the transverse plane at 300 μ m on a cryostat, collected serially onto charged slides (VWR Superfrost plus), and stored at -80°C until microdissection. Slides were placed on a frozen stage (BFS-30MP, Physitemp Instruments) and viewed under a dissection microscope. Tissue was collected directly into RLT lysis Buffer from the RNeasy Micro Plus RNA isolation kit (Qiagen) with a modified 23G needle (inner

diameter = 360 μ m) attached to a syringe and placed on dry ice. The needle was cleaned sequentially between each brain region and sample with RNase away (Invitrogen), 80% ethanol, and RNase-free water. Samples were stored at -80°C until RNA isolation.

We used brain atlases from *A. burtoni* and other fishes to target regions involved in decisions associated with social behaviors. Microdissections were centered on the following nuclei as illustrated in Figure 1: medial part of the dorsal telencephalon (Dm; homologous in part to pallial amygdala); ventral part of the lateral zone of the dorsal telencephalon (Dlv; homologous in part to hippocampus); ventral nucleus of the ventral telencephalon (Vv; homologous in part to lateral septum and external globus pallidus); supracommissural nucleus of the ventral telencephalon (Vs; homologous in part to basal/extended/central amygdala); preoptic area (POA; homologous to preoptic area); anterior tuberal nucleus (ATn; homologous in part to ventromedial hypothalamus); periventricular nucleus of the posterior tuberculum (TPp; homologous in part to dopaminergic A11) (Elliott, Harvey-Girard, Giassi, & Maler, 2017; Goodson & Kingsbury, 2013; Maximino, Lima, Oliveira, Batista, & Herculano, 2012; M. F. Wullimann & Mueller, 2004; Yamamoto & Vernier, 2011). Other important social decision nuclei were not sampled (e.g., periaqueductal gray, PAG;

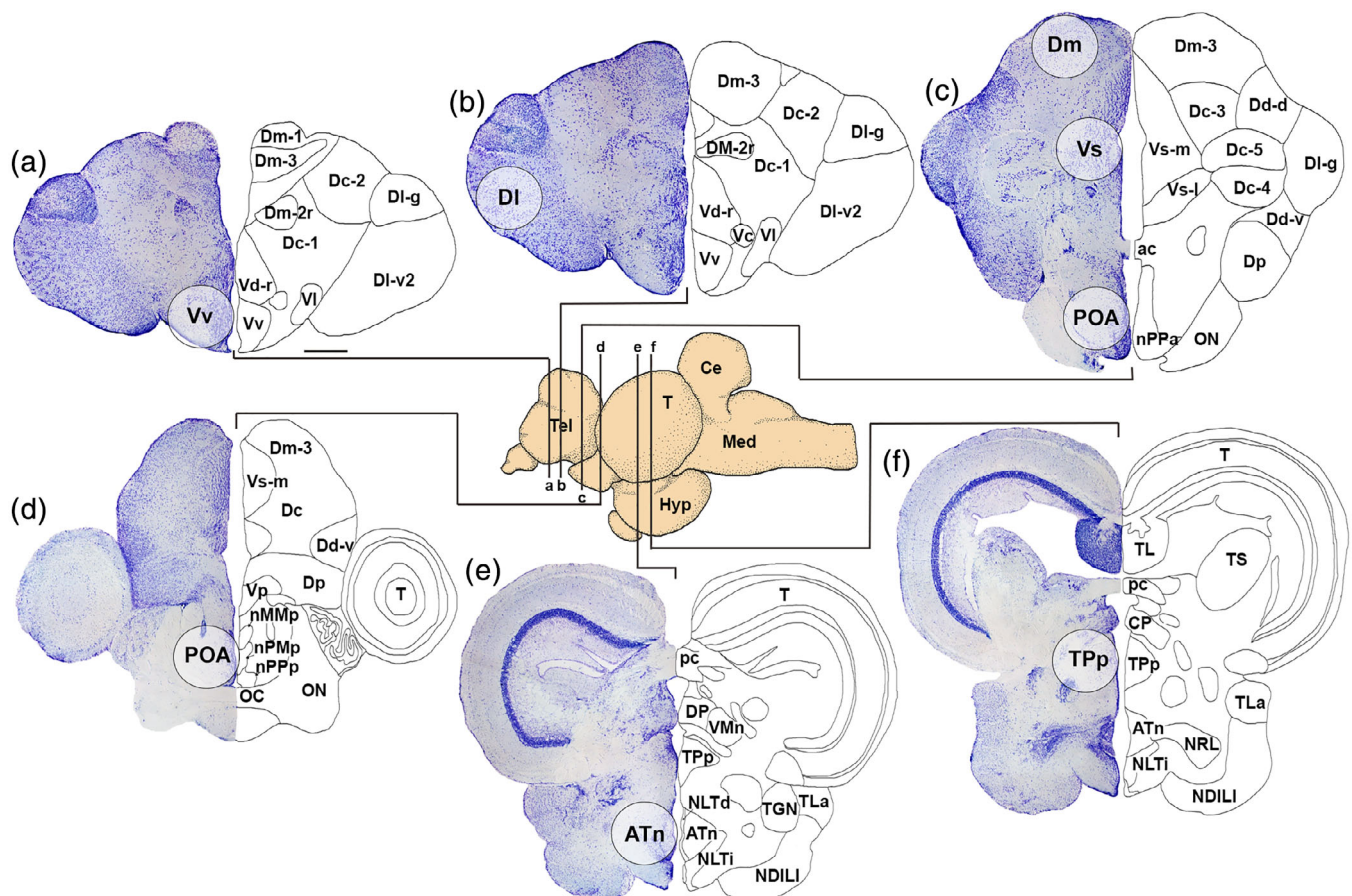


FIGURE 1 Approximate locations of microdissected nuclei in the brain of *Astatotilapia burtoni*. Representative transverse sections stained with cresyl violet (left side) and labeled nuclei (right side) are shown from rostral (a) to caudal (f). Microdissections were centered on specific nuclei (labeled circles) and were collected bilaterally. Center shows a sagittal view of the brain and the approximate locations of each transverse section indicated. See list for abbreviations. Scale bar = 250 μ m [Color figure can be viewed at wileyonlinelibrary.com]

ventral tuberal nucleus, VTn; central part of the ventral nucleus of the ventral telencephalon, Vc; lateral part of the ventral nucleus of the ventral telencephalon, Vl) because they are either too small or difficult to accurately identify in thick sections, which increases the chances of including nontarget regions. We also microdissected the midbrain torus semicircularis (TS; homologous to inferior colliculus; primarily processes auditory and lateral line information, with some visual inputs) and tectum (homologous to superior colliculus; receives visual and other sensory modalities and is involved in sensorimotor integration) to test for changes in estrogen signaling molecules within sensory and sensorimotor processing regions. It is important to note that many of the abovementioned proposed mammalian homologs for these teleost nuclei remain unresolved, particularly in the telencephalon. While collections were centered on the abovementioned nuclei, one limitation of the microdissection technique is that some sampled regions may also contain portions of adjacent nuclei (e.g., ATn may contain portions of lateral tuberal nuclei, Tpp may contain other thalamic regions like CP and DP, and Vv may contain portions of Vc and Vl). Nevertheless, to standardize sampling and reduce variation, all 36 animals were sampled by the same individual and microdissections of each brain region were done sequentially at a single time across all fish before moving to the next brain region. The amount of tissue collected from each brain region was also standardized across all individuals, and included both left and right hemispheres, but differed according to the relative size and extent of each nucleus (two to four 300 μ m microdissected samples per region).

Samples were thawed on ice and vortexed for 30 s, followed by isolation of total RNA according to kit instructions, which includes a step to remove genomic DNA (Qiagen RNeasy Micro Plus). RNA from each sample was then reverse transcribed to cDNA (Quantabio qScript cDNA supermix) and diluted 1:3 with RNase-free water prior to use as a template for qRT-PCR. Quantitative RT-PCR was used to measure mRNA levels of the following candidate genes in microdissected brain regions: estrogen receptors (*era*, *er β a*, *er β b*), brain aromatase (*aromb*; also called *cyp19a1b*), and reference genes *gapdh* and *eef1a*. To examine possible differences in nongenomic effects of estradiol, we also initially measured the membrane-bound G-protein coupled estrogen receptor *gper* (also known as *gpr30*) in the microdissected preoptic area samples of brooding, recovering, and gravid females. In the goldfish, *gper* expression is highest in the preoptic area, but is either absent (e.g., in Vv, Vs, ATn) or expressed at very low levels in the majority of other regions we sampled (Mangiamele, Gomez, Curtis, & Thompson, 2017). Our qPCR measured *gper* at low levels in the POA (late amplification after cycle 35, or errors in calculating the exponential phase), and levels were not different among brooding, recovering, and gravid females (one-way ANOVA, $F_{2,28} = .423$, $p = .659$). Therefore, we did not measure *gper* in any of the other microdissected brain regions. Perfecta SYBR Green Fastmix (QuantaBio) and gene-specific primers (Burmeister, Kailasanath, & Fernald, 2007; Butler et al., 2019; K. P. Maruska, Zhang, et al., 2013) were used for reactions. Quantitative PCR was performed with duplicate reaction volumes of 20 μ l on a CFX Connect System (BioRad). Reaction parameters were 95°C for 30 s, 45 cycles of 95°C for 1 s

and 60°C for 15 s, followed by a melt curve analysis. Fluorescence thresholds for each sample were automatically measured and PCR Miner (Zhao & Fernald, 2005) was used to calculate cycle thresholds and reaction efficiencies for each well. Data were normalized to the geometric mean of the two reference genes, *gapdh* and *eef1a*, as follows: Relative target gene mRNA levels = $[1/(1 + E_{\text{target}})^{CT_{\text{target}}}] / [1/(1 + E_{\text{geomean}})^{CT_{\text{geomean}}}] \times 100$, where E is the reaction efficiency and CT is the average cycle threshold of the duplicate wells. *Gapdh* (glyceraldehyde 3-phosphate dehydrogenase) and *eef1a* (eukaryotic elongation factor 1-alpha) are ubiquitous in all cells and commonly used as reference genes in *A. burtoni* because they are expressed at similar levels independent of fish reproductive condition (Butler et al., 2019; K. P. Maruska, Becker, Neboori, & Fernald, 2013; K. P. Maruska, Zhang, et al., 2013). Levels of *gapdh* and *eef1a* also did not differ among the three female groups for any of the brain regions (all $p > .05$), indicating they are appropriate reference genes for this study. All primer pairs had single melt curve peaks, and sequencing (Eurofins Genomics) from brain tissue in previous studies using identical primers verified they amplified the correct single products.

2.4 | In situ hybridization

Because our qPCR results identified that aromatase differed in many brain regions across female reproductive state, we performed chromogenic in situ hybridization (ISH) to validate our qPCR results and to describe the localization patterns of aromatase throughout the brain. We performed ISH on a total of 15 females (SL: 40.20 ± 3.65 mm; BM: 1.68 ± 0.53 g) comprised of 7 gravid (GSI: 8.01 ± 1.16), 2 recovering (GSI: 5.13 ± 0.28), and 6 mouth brooding (GSI: 0.68 ± 0.15) individuals. Ten of these females were used for *aromb* distribution mapping, 4 were used for double-labels of *aromb* with GFAP (2 gravid, 2 brooding), and 3 were used for double-labels of *aromb* and HuC/D (2 gravid, 1 brooding). Dissected brains were fixed in 4% paraformaldehyde (PFA) made in 1x phosphate-buffered saline (PBS) at 4°C overnight, rinsed in 1xPBS, and cryoprotected in 30% sucrose prepared in 1xPBS for 1–2 days at 4°C. Brains were then mounted in OCT media, sectioned in the transverse plane at 20 μ m with a cryostat, and collected onto alternate charged slides (VWR Superfrost plus). Slides were dried flat at room temperature for 2 days and stored at –80°C until staining.

ISH was done as previously described (Butler & Maruska, 2016; Grone & Maruska, 2015; Porter et al., 2017). Briefly, digoxigenin (DIG)-labeled riboprobes were made from whole brain cDNA with gene-specific *aromb* primers: Forward: 5'-ACAGTAATGTCCTGCTTTGG-3'; Reverse: 5'-CGTGAGGTTGAAGTCTTTAGG-3'. Purified probes were diluted and stored at –20°C until use. Sense control probes were generated in the same manner but had the T3 recognition sequence (aattaaccctcactaaaggg) added to the forward (sense) primer. Slides of cryosectioned brains were brought to room temperature and tissue was surrounded with a hydrophobic barrier (Immedge pen, Vector Laboratories). Slides were treated with the following solutions: 1xPBS (3 \times 5 min), 4% PFA (20 min), 1xPBS (2 \times 5 min), proteinase K (10 min),

1×PBS (10 min), 4% PFA (15 min), 1×PBS (2 × 5 min), milliQ water (3 min), 0.1 M triethanolamine-HCl pH 8.0 with acetic anhydride (10 min), 1×PBS (5 min). Slides were then prehybridized (hybridization buffer without probe) for 3 hr in a sealed chamber at 60–65°C, followed by replacement with probe solution (probe in hybridization buffer). Slides with DIG-labeled probe solution were covered with hybridization buffer and hybridized overnight (~18 hr) in a 60–65°C oven. After hybridization, stringency washes were performed at 60–65°C as follows: 2× saline sodium citrate (SSC): 50% formamide (2 × 30 min), 1:1 mixture of 2× SSC: maleate buffer with tween (MABT; 2 × 15 min), and MABT (2 × 10 min). Slides were transferred to room temperature and washed with MABT (2 × 10 min), followed by blocking of nonspecific binding with MABT containing 2% bovine serum albumin (BSA) for 3 hr at room temperature. After blocking, slides were incubated with anti-DIG AP antibody (Roche; diluted 1:5,000 in blocking solution) overnight at 4°C in a sealed humidified chamber. Slides were then washed in MABT (3 × 30 min), treated with alkaline phosphatase (AP) buffer (2 × 5 min), and developed in NBT/BCIP solution at 37°C for 5 hr. Following development, slides were treated in the following solutions: 1×PBS (3 × 5 min), 4% PFA (10 min), 1×PBS (3 × 5 min). Slides were coverslipped with aqueous mounting media (Aquamount, Lerner Laboratories), dried flat overnight, and then edges sealed with clear nail polish.

2.5 | Double fluorescent ISH-IHC

To test whether *aromb* was expressed in radial glial cells, as seen in other teleost fishes, we also performed double fluorescent ISH for *aromb* mRNA and immunohistochemistry (IHC) for the radial glial marker GFAP (glial fibrillary acidic protein) or the RNA-binding protein neuronal marker HuC/HuD. Slides were first stained for *aromb* mRNA using the chromogenic ISH protocol described above, but were developed using Sigma-Fast Red instead of NBT/BCIP as a substrate and subsequent steps were performed in the dark. The reaction was stopped with 1×PBS washes (4 × 10 min) at RT, nonspecific binding was blocked by incubation in 1×PBS containing 5% normal goat serum, 0.2% BSA, and 0.3% Triton-X for 2 hr at room temperature. Slides were then incubated with mouse monoclonal anti-GFAP (GA5, #3670, Cell Signaling Technology; 1:300; RRID: AB_561049) or mouse monoclonal anti-HuC/HuD [16A11] (#A21271, Invitrogen, 1:200; RRID: AB_221448) at 4°C for 12–16 hr. Slides were washed in 1×PBS (3 × 10 min), incubated in Alexa Fluor 488 goat anti-mouse secondary antibody (#A11029, Invitrogen, 1:400 in 1×PBS with 10% normal goat serum) for 2 hr, and washed in 1×PBS (3 × 10 min). Slides were coverslipped with Fluorogel II containing DAPI (Electron Microscopy Services, Hatfield, PA) to label cell nuclei.

2.6 | Antibody characterization

Glial fibrillary acidic protein (GFAP) is an intermediate filament protein found in several cell types of the central nervous system in vertebrates,

including astrocytes and radial glial cells. The mouse monoclonal anti-GFAP (GA5, #3670, Cell Signaling Technology; RRID: AB_561049) was produced by immunizing animals with native GFAP purified from pig spinal cord. In *A. burtoni*, this antibody labels the cytoplasm of cells with the characteristic morphology and localization of radial glial cells seen in other teleost fishes (Forlano et al., 2001; Tong et al., 2009), stains a single band of the appropriate molecular weight (~50 kDa) in western blots run on protein isolates of whole *A. burtoni* brains, and was identical to staining seen in our previous study in this species (K. P. Maruska, Carpenter, & Fernald, 2012). Omission of primary antibody or secondary antibody resulted in no staining (K. P. Maruska, Carpenter, et al., 2012).

The HuC/D antiserum was mouse monoclonal anti-HuC/HuD (16A11) (#A21271, Invitrogen), produced from a synthetic peptide representing amino acids 240–251 within the carboxy-terminal domain of human HuD, which labels the Elav family of neuronal proteins, HuC, HuD, and Hel-N1. This antibody was previously shown to label neuronal cells in zebrafish, chick, canaries, and humans (Ampatzis & Dermon, 2011; Barami, Iversen, Furneaux, & Goldman, 1995; Marusich, Furneaux, Henion, & Weston, 1994; Wakamatsu & Weston, 1997). In *A. burtoni*, it only stained the cytoplasm of cells with the characteristic morphology and distribution of neurons, and was identical to that observed in our previous study in this species (K. P. Maruska, Carpenter, et al., 2012). Omission of primary antibody or secondary antibody during immunohistochemistry resulted in no staining (K. P. Maruska, Carpenter, et al., 2012).

2.7 | Imaging and analysis

To map the distribution of *aromb*-expressing cells, slides of stained tissue were visualized on a Nikon Eclipse Ni microscope controlled by Nikon Elements software (RRID:SCR_014329), and photographs were taken with either a color digital camera (Nikon DS-Fi2) for chromogenic-ISH, or a monochrome digital camera (Nikon DS QiMc) for double fluorescent ISH-IHC. Images were adjusted for contrast, brightness, and levels as needed in Photoshop (Adobe Systems, San Jose, CA; RRID: SCR_014199) or ImageJ (imagej.nih.gov/ij/; RRID: SCR_003070). In some cases, distracting artifacts were also removed with the Photoshop clone tool. Fluorescent images were pseudocolored and merged in ImageJ. To facilitate identification of neuroanatomical structures and brain nuclei, we used a cresyl-violet stained *A. burtoni* reference brain and annotated atlas, as well as other brain atlases from this and other teleost species (Burmeister, Munshi, & Fernald, 2009; Fernald & Shelton, 1985; K. P. Maruska, Butler, Field, & Porter, 2017; Munoz-Cueto, Sarasquete, Zohar, & Kah, 2001; M.F. Wullmann, Rupp, & Reichert, 1996).

2.8 | Statistical analysis

Comparisons of SL, BM, GSI, and circulating steroid levels (E2, 11KT) were made with one-way analysis of variance (ANOVA) followed by post hoc Student–Newman–Keuls (SNK) tests. Outliers were removed prior to analysis (Grubb's outlier test), and data that did not meet assumptions of normality or equal variance were first log transformed.

mRNA levels of each candidate gene were compared with general linear mixed models, with brain region as within-subject factors, reproductive state as between-subject factors, and body mass as a covariate, followed by post hoc pairwise comparisons (SNK). Correlation analyses were performed with Pearson correlation tests, and Benjamini-Hochberg procedure was used to correct for multiple comparisons with a false discovery rate of 5%. Hierarchical clustering (Ward linkage, standardized values) was used to determine *aromb* clusters based on Pearson correlation coefficients displayed in a heat map. Discriminant function analysis (DFA) was used to test whether gene expression could predict grouping of females into their correct reproductive states. Principal component analysis (PCA) was performed on aromatase expression data across brain regions using Eigenvalues >1, missing values excluded list-wise, and components plotted in rotated (varimax) space. All data were analyzed in SigmaPlot 12.3 or IBM SPSS 25.

3 | RESULTS

3.1 | GSI and plasma sex-steroid hormones

All three female groups had statistically different GSIs (one-way ANOVA, $F_{2,33} = 303.84$, $p < .001$; post hoc SNK, all $p < .001$) with highest values in gravid, followed by recovering, and then brooding females with the lowest (Figure 2a). Gravid females also had higher circulating E2 levels than both recovering and brooding (one-way ANOVA, $F_{2,31} = 30.68$, $p < .001$; SNK, $p < .001$) females, and recovering females had higher E2 levels than brooding (SNK, $p = .043$) females (Figure 2b). Circulating 11KT levels were higher in gravid females

(one-way ANOVA, $F_{2,32} = 20.85$, $p < .001$) compared to both recovering and brooding females (SNK, $p < .001$), but brooding and recovering did not differ (SNK, $p = .988$) (Figure 2c). When all fish are examined together, serum levels of all E2 and 11KT are positively correlated ($r = .703$, $p < .01$), and plasma steroids are positively correlated with GSI (E2, $r = .748$, $p < .001$; 11KT, $r = .681$, $p < .001$).

3.2 | Localization of aromatase expression in the brain

To localize regions of aromatase expression throughout the brain of *A. burtoni*, we performed chromogenic ISH with riboprobes. Aromatase-expressing cells were consistently found bordering the brain ventricles from the forebrain to the hindbrain (Figures 3 and 4), while tissue treated with sense control probes showed no staining (Figure 5).

3.2.1 | Olfactory bulbs and telencephalon

In the olfactory bulbs, scattered *aromb*-stained cells and fibers are found throughout the glomerular cell layer of the olfactory bulb (GL, Figure 3a and 4a). A few stained cells also lie in the internal cell layer of the olfactory bulb (ICL) and along the dorsomedial edge of the ICL. Throughout the telencephalon, *aromb*-staining was dense along the medial ventricular edge, especially in subpallial regions (e.g., dorsal, postcommissural, supra commissural, and ventral parts of ventral telencephalon; Vd, Vp, Vs, and Vv; Figures 3b–e and 4a–c). A few stained cells are located off the midline in Vv and Vd (Figure 3b). Cellular projections away from the midline are also present throughout Vd, Vs, and Vv. Expression was also

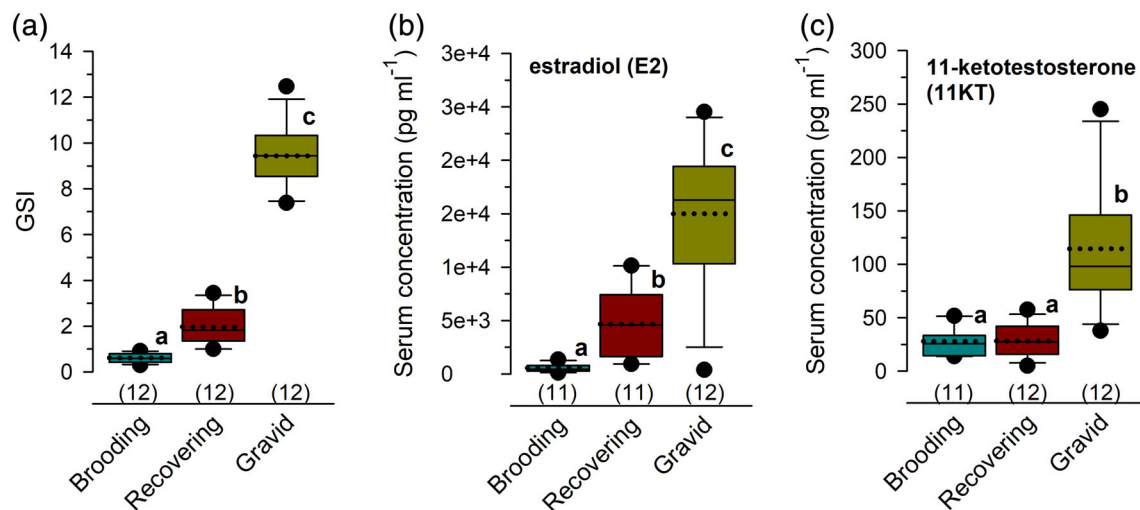


FIGURE 2 Gonadosomatic index and circulating sex-steroid levels differ with female reproductive state in *A. burtoni*. (a) Gonadosomatic index (GSI), a measure of reproductive investment, differed among gravid, recovering, and brooding females. (b) Circulating estradiol levels differ among all three female groups, and increase with gravidity. (c) Levels of 11-ketotestosterone were higher in gravid females compared to both brooding and recovering females. Sample sizes (number of fish) are shown in parentheses. Boxes extend to the furthest points within the 25th and 75th percentiles, and whiskers to the 10th and 90th percentiles. The median is represented by a solid line, mean as a dotted line, and any data points outside the 10th–90th percentiles are shown as filled circles. Different letters indicate statistical significance at $p < .05$ [Color figure can be viewed at wileyonlinelibrary.com]

seen at the external brain surface in the pallial telencephalon in the regions of Dm and DI (Figure 3a–d and 4a,b). Because the teleost telencephalon develops by eversion rather than invagination as in tetrapods, these Dm and DI surfaces border the ventricle that is located

surrounding the pallial regions. In the rostral telencephalon, dense *aromb* staining is found along the ventral edges of the ventral part of the lateral zone of the dorsal telencephalon (DI-v; Figure 3a,b and 4a,b). Only a few scattered cells are present along the dorsolateral edges (e.g., medial part

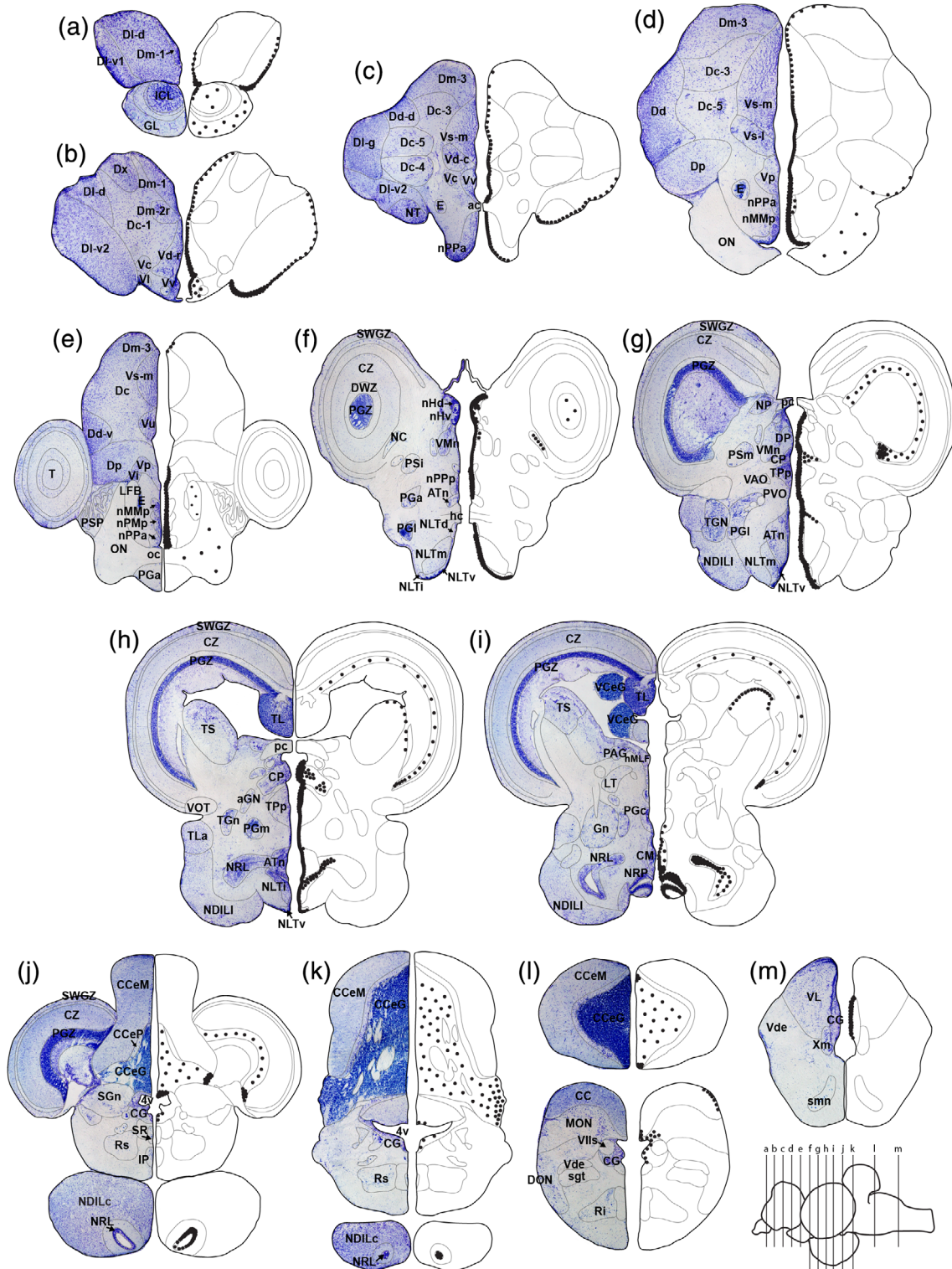


FIGURE 3 Aromatase is expressed primarily along ventricular borders from olfactory bulbs to hindbrain. Left side of each panel depicts a cresyl violet-stained brain section with approximate regions outlined. Right side of each panel shows localization of *aromb*-expressing cells (dots) revealed by chromogenic ISH. Number of dots represents relative staining density. Approximate locations of transverse sections shown rostral (a) to caudal (m) are depicted in inset in bottom right corner. See list for abbreviations [Color figure can be viewed at wileyonlinelibrary.com]

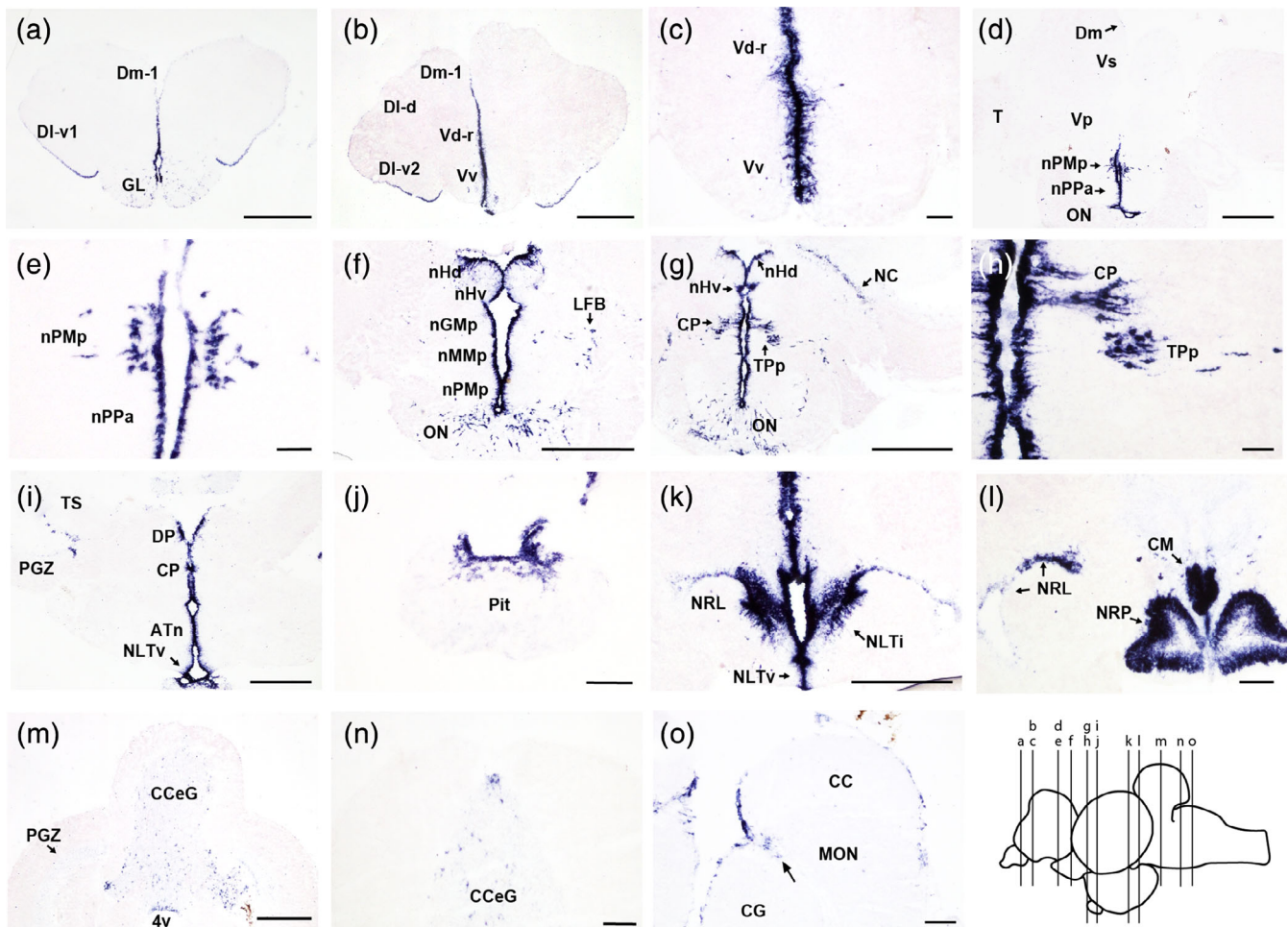


FIGURE 4 Representative photomicrographs of *aromb* ISH staining throughout the female *A. burtoni* brain. Aromatase expression is observed along ventricular borders from the olfactory bulbs to the hindbrain. Approximate locations of transverse sections shown rostral (a) to caudal (o) are depicted in inset in bottom right corner. Arrow in o denotes *aromb* expression off the midline in MON. Scale bars = 500 μ m in a, b, d, f, g, i, k, m; 100 μ m in c, j, l, n, o; 50 μ m: e, h. See list for abbreviations [Color figure can be viewed at wileyonlinelibrary.com]

of the dorsal telencephalon, Dm; Figure 3d). This staining was consistently lighter and absent of obvious cellular projections when compared to medial ventricular edge staining.

3.2.2 | Diencephalon

Abundant *aromb* expression occurs along the ventricular midline throughout the diencephalon (Figures 3 and 4). It is especially dense in the area of the preoptic area, where some cells have migrated away from the midline (i.e., nPMp) and cellular extensions off the midline are observed (Figures 3d,e and 4d,e). In addition, scattered cells are found in the optic nerve and lateral forebrain bundle (LFB; Figures 3d,e and 4f,g). Aromatase expression is also present throughout both ventral and dorsal habenula (nHv, nHd) and along the midline ventricle throughout rostral thalamic regions, including ventromedial thalamic nucleus (VMn), central and dorsal posterior thalamic nuclei (CP, DP), periventricular nuclei of the posterior tuberculum (TPp), and paraventricular organ (PVO) (Figures 3f–h and

4f–i). In the area of CP and TPp, *aromb*-expressing cells are also located off the midline in two distinct clusters and radial fiber projections are also found in this region (Figure 4h). In the hypothalamus, *aromb* is present along the midline in the anterior and lateral tuberal nuclei (ATn, NLT; Figures 3f–h and 4i,k). A few stained cells are observed off the midline at the ventral border of ATn and throughout the intermediate part of NLT (NLTi) extending towards the nucleus of the lateral recess (NRL). In addition, *aromb*-expressing cells lie in the NRL along ventricular edges, especially the dorsal, medial portion (Figures 3h,i and 4k,l). A few cells are found in the nucleus corticalis (NC; Figures 3f and 4g), while abundant *aromb* staining is found along the medial ventricular edge in the area of corpus mammillare (CM) and ventral commissural preglomerular nucleus (PGc) with a few large stained cells located off the midline (Figure 3i and 4l). The nucleus of the posterior recess (NRP) is also densely stained with *aromb* (Figures 3i and 4l). *Aromb*-expressing cells also lie in the pituitary, and are notably dense in the neurohypophysis (Figure 4j), but also occur scattered throughout the different regions of the adenohypophysis.

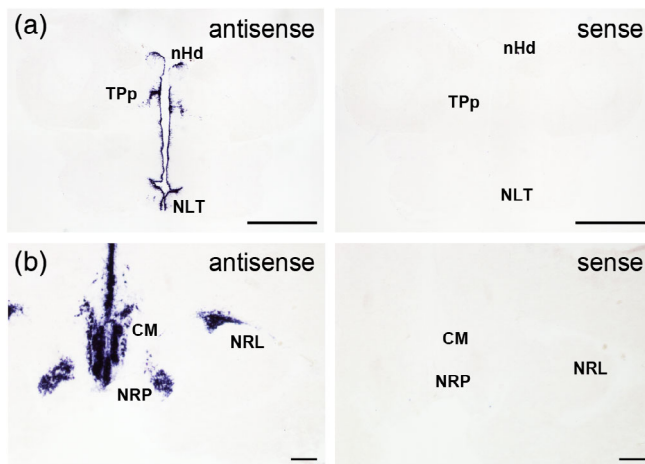


FIGURE 5 Representative examples of chromogenic ISH staining in coronal brain sections of *A. burtoni* to illustrate *aromb* probe specificity. Low (a) and high (b) magnification of antisense (AS; left) and sense (S; right) control probes on alternate sections within diencephalic regions of the same brain. Scale bars = 1,000 μm in a; 100 μm in b. See list for abbreviations [Color figure can be viewed at wileyonlinelibrary.com]

3.2.3 | Mesencephalon and rhombencephalon

Compared to the forebrain, *aromb*-expressing cells are less abundant in the mesencephalon and rhombencephalon. The dense *aromb* expression so prominent along the ventricular midline in the diencephalon diminishes and disappears in the midbrain, with no/few *aromb*-expressing cells along the midline in the tegmental regions (Figure 3i). There are, however, scattered *aromb*-expressing cells located dorsally in the torus semicircularis (along the TSc) bordering the cerebral aqueduct (TS; Figures 6c and 3h,i) and in the periventricular gray zone of the tectum (PGZ; Figures 6c and 3f-j).

In the cerebellum, *aromb*-stained cells and fibers lie in the granular layer of corpus cerebellum (CCeG), with a higher density of cells in the lateral portion (Figures 3j-l and 4m,n). Higher density staining is found in the ventral and dorsal tips of the CCeG in the caudal cerebellum, an area where cell proliferation occurs (K. P. Maruska, Carpenter, et al., 2012) (Figure 3n). *Aromatase* expression is also found along the edge of the fourth ventricle (4v; Figures 3k-l and 4m,o) in the central gray (CG) and, more caudally, along the midline of the CG (Figure 3j-m). In the cerebellar crest (CC), scattered cells lie along the medial and lateral edges (Figure 3l and 4o). Cells and fiber projections off the midline are present in the medial octavolateralis nucleus (MON) (Figures 3l and 4o, arrow). No *aromb* expression was found in the spinal cord.

3.2.4 | Female reproductive-state differences in *aromb* ISH staining

Aromb-staining was more abundant throughout the brain of gravid females compared to mouth brooding females (Figure 7). Midline ventricular staining along subpallial regions (e.g., Vv, Vs) is darker and

appeared to have more stained cellular projections in gravid females (Figure 7a-c). Pallial regions of brooding females also have reduced *aromb*-staining along ventricular edges (Figure 7b) and staining was absent along the Dm border of all brooding females. In the preoptic area and CP/TPp, the *aromb*-stained cell groups that are located off the midline were more densely stained and appeared to contain a greater number of cells and radial projections in gravid compared to brooding females (Figure 7c-e). In the hindbrain, gravid females also had more staining in the regions of the MON and CC (Figure 7f). Throughout the diencephalon, mesencephalon, and rhombencephalon, aromatase staining is also lighter and with fewer projections in brooding compared to gravid females.

3.3 | Aromatase is co-localized with the radial glial marker GFAP, but not the neuronal marker HuC/D

Aromatase expression is predominantly found in areas where glial cells are located (K. P. Maruska, Carpenter, et al., 2012). To determine if aromatase is expressed in glial cells, we performed a double fluorescent label for *aromb* and the radial glial cell marker GFAP (Figure 8). The majority of *aromb* staining is found in areas where radial glia cell bodies and projections are located, especially along ventricular borders (Figure 8), and co-labeling of *aromb* and GFAP in the same cells was observed in many regions. The only exception is found in the *aromb*-labeled cells that have migrated away from the midline in the POA and thalamic CP/TPp area where *aromb* and GFAP do not co-localize (Figure 8b-d). To exclude the possibility that these cells are neurons, we also performed a double fluorescent label for *aromb* and the neuron marker anti-HuC/D (Figure 9). There was no co-labeling of *aromb* and HuC/D in the same cells. Along the ventricles, *aromb*-expressing cells lie directly along the midline ventricular surface, while HuC-D positive cells lie predominantly more lateral to this and off of the ventricular surface. In addition, no *aromb*-labeled cell bodies co-localized with anti-HuC/D in the POA or CP/TPp regions (Figure 9), but *aromb*- and HuC/D-expressing cells were intermingled in the same regions of the POA and TPp (Figure 9b-d). Thus, the *aromb*-expressing cells located off of the ventricular midline in POA and TPp do not express either GFAP or HuC/D, so their cellular identity is unclear.

3.4 | Expression levels of estrogen signaling molecules across female reproductive state

3.4.1 | Expression levels in social behavior nuclei

There were no differences among brooding, recovering, and gravid females in any brain region for *era* (GLM $F_{2,34} = 1.47$, $p = .176$), *er β a* ($F_{2,34} = 1.63$, $p = .100$), or *er β b* ($F_{2,33} = .620$, $p = .835$) mRNA levels (Figure 10). In contrast, *aromb* expression did differ among female groups in all tested brain regions (GLM $F_{2,34} = 4.6$, $p < .001$) (Figure 11). In Dm and DI, *aromb* levels were higher in gravid females compared to both recovering and brooding females, which did not

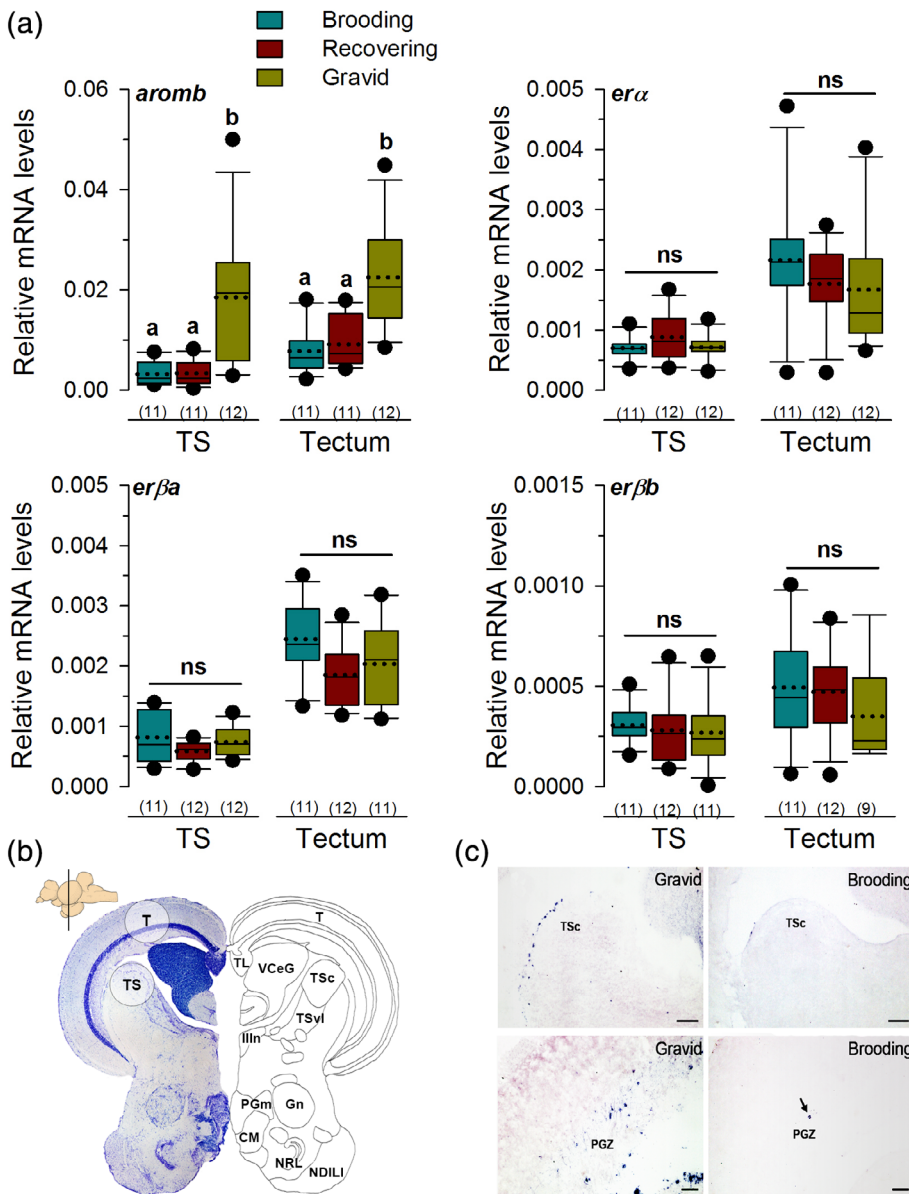


FIGURE 6 Aromatase, but not estrogen receptor, expression in the midbrain torus semicircularis and tectum varies with female reproductive state. (a) mRNA levels of *aromb* in the TS and tectum were greater in gravid compared to both recovering and brooding females. mRNA levels of *er α* , *er β a*, and *er β b* did not differ with reproductive state in TS or tectum. Data are expressed relative to the geometric mean of the reference genes. Ns, not significant at $p > .05$. Different letters indicate statistical differences at $p > .05$. See Figure 3 for box plot descriptions. (b) Representative transverse section stained with cresyl violet (left side) and labeled nuclei (right side) to illustrate microdissection location of TS and T (labeled circles) used for qPCR. Inset shows a sagittal view of the brain and the approximate location of the transverse section is indicated. (c) Example staining of *aromb* in torus semicircularis and periventricular gray zone (PGZ) of the tectum in gravid (left) and brooding (right) females. Scale bars = 100 μ m (top TS images); 50 μ m (bottom PGZ images). See list for abbreviations [Color figure can be viewed at wileyonlinelibrary.com]

differ from each other (Table 2). In Vs, POA, and ATn, both gravid and recovering females had higher *aromb* levels compared to brooding females (Table 2). In Vv and Tpp, *aromb* levels were statistically different among all three female groups in the order gravid > recovering > brooding (Figure 11, Table 2).

Because the only difference in gene expression among female reproductive states was in *aromb*, we further explored aromatase expression by performing Pearson correlations to generate a heat map of expression among brain regions in all animals together, and used hierarchical cluster analysis (Ward linkage) to group brain regions based on these correlations (Figure 11b). This analysis revealed two main clusters of *aromb* co-expression: one of Vv, Vs, POA, ATn, and Tpp, and a second of Dm and Dl. Principal component analysis on *aromb* expression in all microdissected brain regions also extracted two components that explained 67.87% of the total variance (KMO = 0.759; Bartlett's test chi-square = 77.89; $df = 21$; $p < .001$)

(Figure 11c). Component 1 explained 49.87% of the variance and was loaded by aromatase expression in the subpallial telencephalic regions Vv and Vs together with the diencephalic regions POA, ATn, and Tpp. Component 2 explained 17.99% of the variance and was loaded by *aromb* expression in the pallial regions Dm and Dl. Thus, the hierarchical clustering and PCA both revealed the same two separate co-expression brain networks based on *aromb* levels: a subpallial and diencephalic network of Vv, Vs, POA, ATn, and Tpp, and a pallial network (Dm and Dl).

Discriminant function analysis was also used to test whether *aromb* expression across all microdissected regions could accurately predict female reproductive state (Figure 11). The DFA produced one significant function (Function 1; Eigenvalue = 5.437; chi-square = 43.070; $df = 14$; $p < .001$) that explained 96.3% of the total variance and correctly classified 86.1% of females into their respective groups (brooding: 91.7%, recovering: 75.0%, gravid: 91.7%)

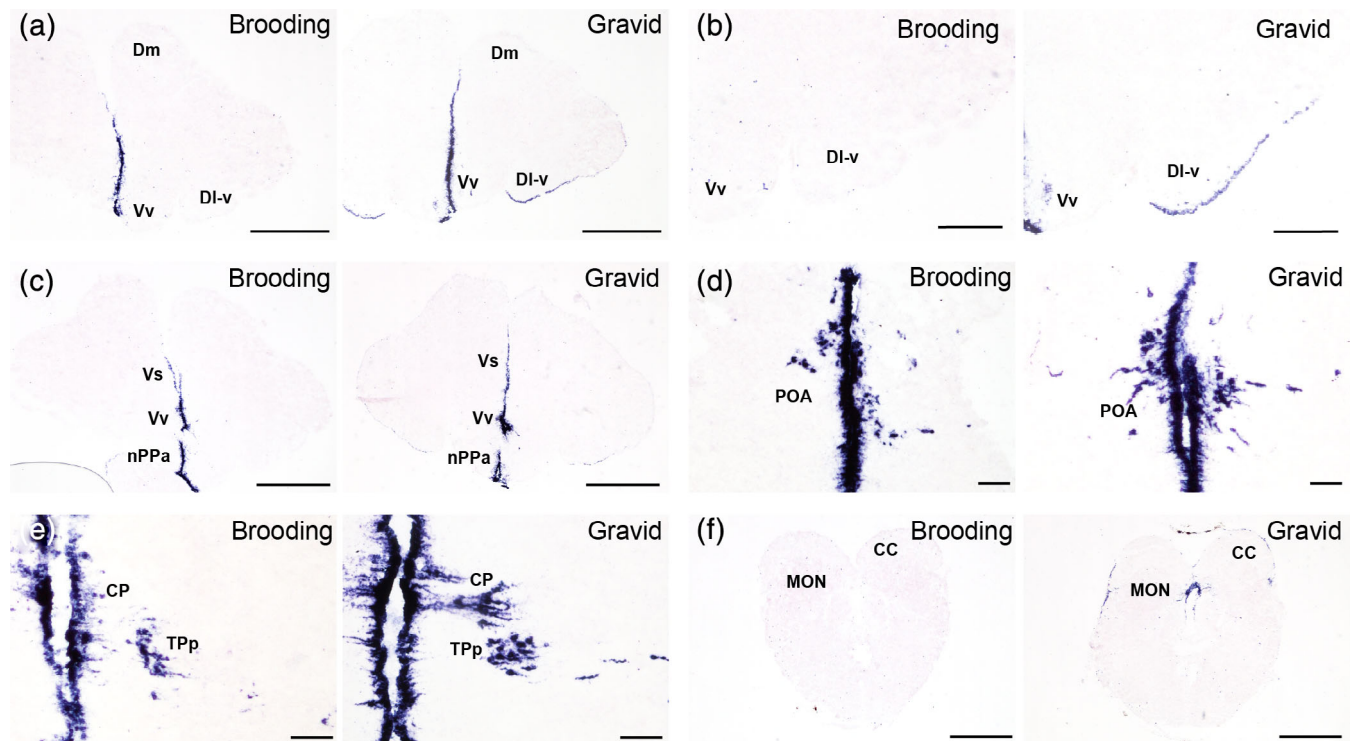


FIGURE 7 Aromatase staining is denser and more widespread in gravid females compared to mouth brooding females. Representative photomicrographs of aromatase ISH staining in the telencephalon (a, b, c), preoptic area (c, d), thalamus (e), and hindbrain (f) of mouth brooding (left images) and gravid (right images) female brains. Scale bar = 500 μm in a, c, f; 250 μm in b; 100 μm in e; 50 μm in d. See list for abbreviations [Color figure can be viewed at wileyonlinelibrary.com]

(Figure 11d). In contrast, DFAs on the expression of estrogen receptors were unable to correctly classify female reproductive state (all $p > .05$).

To examine whether gene expression in each brain region was related to female reproductive state, we tested for correlations with GSI and circulating steroid levels. *Aromb* levels were positively correlated with GSI in all brain regions (Table 3). *Aromb* levels were also positively correlated with circulating levels of E2 in all brain regions (Figure 12; Table 3), and with 11KT in DI, Vv, ATn, and TPp. Levels of *era* were positively correlated with GSI only in Vv ($r = .50$, $p = .003$) and ATn ($r = .41$, $p = .015$). Levels of *era* were not correlated with circulating E2 in any brain region (all $r < .30$, $p > .05$). There were no correlations between GSI and *er β a* or *er β b* in any brain region (all $p > .05$). There were also no significant correlations between *er β a* or *er β b* levels in any brain region with circulating E2 (all $p > .05$). Thus, aromatase expression throughout the brain appears closely tied to female gonadal state and circulating estradiol (and circulating 11-KT in some brain regions), while expression of brain estrogen receptors does not.

We next tested whether *aromb* expression correlated with expression of estrogen receptors (*era*, *er β a*, *er β b*) within the same brain region across all animals together. This analysis yielded only two significant positive correlations between *aromb* and *era* in POA ($r = .46$, $p = .005$) and TPp ($r = .45$, $p = .007$). Within a particular brain region, therefore, there is little to no relationship between

aromatization capacity and expression of estrogen receptors that would bind the localized production of estradiol.

3.4.2 | Expression levels in sensory and sensorimotor midbrain nuclei

In addition to forebrain regions involved in social behaviors, we also tested whether genes involved in estrogen signaling varied across the female reproductive cycle within midbrain sensory and sensorimotor processing regions (Figure 6). In the torus semicircularis, mRNA levels of *aromb* were higher in gravid compared to both brooding and recovering females (GLM $F_{2,33} = 10.47$, $p < .001$), but brooding and recovering did not differ from each other (Figure 6a; Table 2). Estrogen receptor mRNA levels in TS did not differ with female reproductive state (GLM *era* $F_{2,33} = .74$, $p = .487$; *er β a* $F_{2,33} = 2.25$, $p = .121$; *er β b* $F_{2,31} = 1.10$, $p = .343$) (Figure 6a). In TS, *aromb* levels were also positively correlated with plasma E2 and 11KT levels (Table 3), but estrogen receptors were not correlated with either sex-steroid (all $r < .30$, $p > .20$). GSI was also positively correlated with TS *aromb* levels, but not estrogen receptors (all $r < .20$, $p > .35$).

In the tectum, mRNA levels of *aromb* were higher in gravid compared to both brooding and recovering females (GLM $F_{2,31} = 14.56$, $p < .001$), but brooding and recovering did not differ from each other (Figure 6a). Estrogen receptor mRNA levels in the tectum also did not

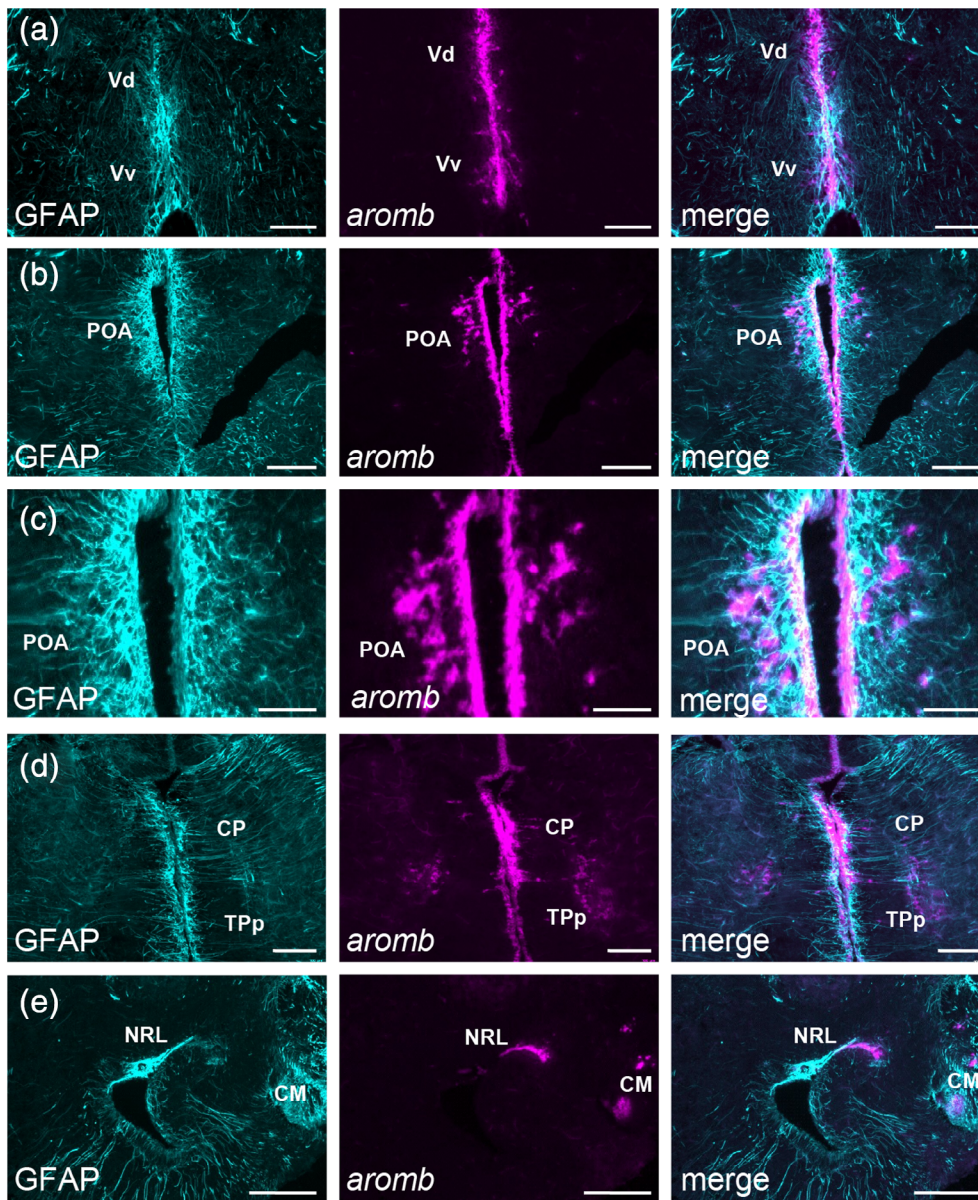


FIGURE 8 Aromatase expression is predominantly found co-localized in radial glial cells labeled by GFAP. Co-localization of GFAP (cyan, left column) and *aromb* (magenta, middle column) indicates aromatase expression is predominantly found in radial glial cells located on ventricular edges (merged images in right column). Representative examples in subpallial ventral telencephalic areas along the midline (a), preoptic area (b and c), thalamus (c), and hypothalamus (d) show *aromb*-stained cell groups co-localized with GFAP. Scale bar = 250 μm in e; 100 μm in a, b, d; 50 μm in c. See list for abbreviations [Color figure can be viewed at wileyonlinelibrary.com]

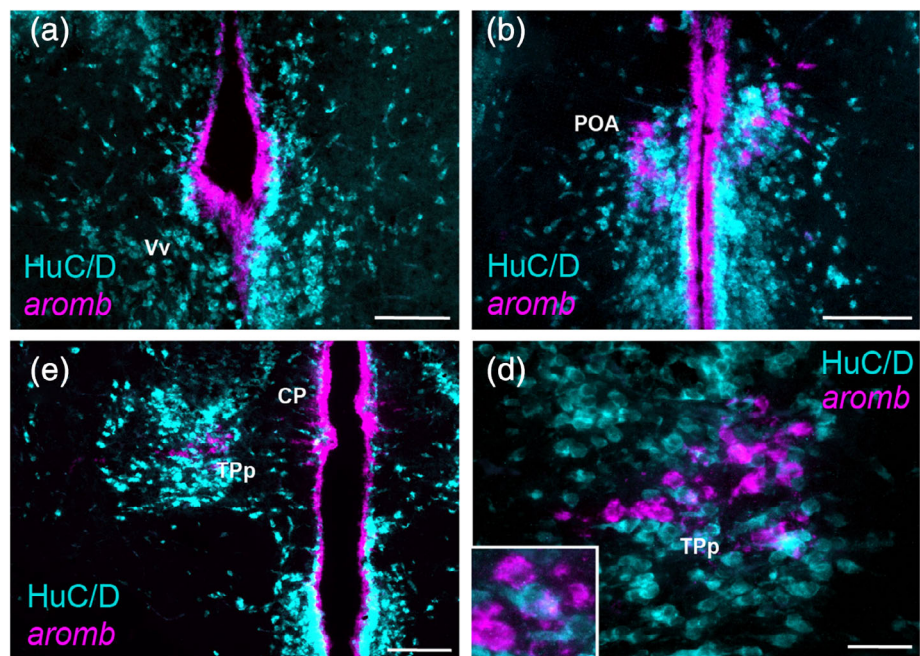
differ with female reproductive state (GLM $er\alpha$ $F_{2,32} = .833$, $p = .444$; $er\beta\alpha$ $F_{2,31} = 2.85$, $p = .073$; $er\beta\beta$ $F_{2,29} = .955$, $p = .396$) (Figure 6a). Plasma estradiol was positively correlated with tectum *aromb* levels, but 11KT was not (Table 3). Tectum estrogen receptors were not correlated with circulating estradiol (all $r < .20$, $p > .15$). GSI was also positively correlated with tectum *aromb* levels, but not estrogen receptors (all $r < .20$, $p > .33$). Thus, similar to the social decision regions, aromatase expression in the midbrain torus semicircularis and tectum is correlated with female gonadal state and circulating estradiol, while expression of estrogen receptors is not.

4 | DISCUSSION

We used the nonseasonally breeding and maternal mouth brooding African cichlid fish *A. burtoni* to examine reproductive-state changes

in estrogenic signaling (aromatase and estrogen receptors) within localized regions of the female brain. Our results demonstrate that mRNA expression levels of the rate-limiting enzyme aromatase, but not estrogen receptors, change across the reproductive cycle. Gravid females that are close to spawning had higher aromatase levels in all brain regions compared to females with lower reproductive potential that were either recovering or mouth brooding. This brain aromatase expression was positively correlated with GSI and circulating estradiol levels. Using ISH, we also localized aromatase-expressing cells primarily to small ependymal cells along the ventricles throughout the brain, and observed more intense staining in gravid compared to mouth brooding females in most regions. Aromatase expression was primarily found in radial glial cells, shown by co-localization with the glial marker GFAP. These results highlight the importance of estrogen synthesis throughout the female *A. burtoni* brain during the reproductive cycle, with potential functional implications for ovarian readiness,

FIGURE 9 Aromatase is not co-localized with the neuronal marker HuC/D. *Aromb*-expressing cells located along the ventricle borders in the ventral telencephalon (a), preoptic area (b), and periventricular nucleus of the posterior tuberculum (c and d) did not co-localize with the neuron marker HuC/D. *Aromb*-expressing cells located off of the ventricular midline were intermingled with HuC/D-labeled cells (b–d), but did not appear to co-localize in the same cells with either HuC/D or GFAP. Scale bar = 100 μ m in a, b, c; 25 μ m in d. See list for abbreviations [Color figure can be viewed at wileyonlinelibrary.com]



sexual motivation, sensory perception, neurogenesis, and behavioral decisions associated with mate choice and spawning.

5 | DISTRIBUTION OF AROMATASE-EXPRESSING CELLS IN THE *A. BURTONI* BRAIN

Similar to other teleost fishes examined to date, the cichlid *A. burtoni* had abundant aromatase-expressing cells in the ependymal regions associated with the ventricle borders. Relative levels of aromatase revealed by both ISH and qPCR showed the most abundant expression in telencephalic subpallial areas along the midline ventricle, and diencephalic areas of the preoptic area, thalamus, and hypothalamus associated with the 3rd ventricle and lateral recess. This pattern, along with significant expression in olfactory bulbs and pallial ventricular regions of the dorsal telencephalon, is also similar to other examined teleosts (Table 1). In contrast, it appears that more caudal brain regions (e.g., midbrain, hindbrain, cerebellum) show more variation in aromatase expression among fish species (Table 1). For example, we observed aromatase expression in the midbrain torus semicircularis (homologous to mammalian inferior colliculus), which is absent in the midshipman (Forlano et al., 2001) and brown ghost knifefish (Shaw & Krahe, 2018), but present in some other species [e.g., rainbow trout (Menuet et al., 2003), zebrafish (Goto-Kazeto et al., 2004), bluehead wrasse (Marsh et al., 2006)]. Similarly, we detected aromatase expression in the midbrain tectum (homologous to mammalian superior colliculus), which exists in other fishes, but is also absent in the midshipman and brown ghost knifefish (see Table 1). The torus semicircularis is an important processing center for auditory and lateral line information (and may also receive visual and somatosensory inputs) and the tectum is involved in visual and multisensory

processing, as well as sensorimotor integration. Female *A. burtoni* rely on multimodal sensory information (visual, auditory, mechanosensory, chemosensory) from courting dominant males to coordinate their mate choice and spawning activities (Butler et al., 2019; Field & Maruska, 2017; K. P. Maruska & Fernald, 2012, 2018; Maruska et al., 2012). Thus, modulation of neural processing and circuitry by estrogens in these nuclei may facilitate sensory perception and reproductive behaviors. It is well-documented in songbirds, for example, that local estrogen signaling in the brain influences both song production and auditory sensitivity related to seasonal breeding activities (Ramage-Healey, Coleman, Oyama, & Schlinger, 2010; Ramage-Healey, Jeon, & Joshi, 2013; Ramage-Healey, Oyama, & Schlinger, 2009), and the abundant aromatase expression in the sonic motor nucleus of the midshipman fish suggests modulation of reproductive-related sound production (Forlano et al., 2001; Forlano & Bass, 2005; Forlano, Deitcher, & Bass, 2005; Ramage-Healey & Bass, 2007). Local estrogen production by aromatase positive ganglion neurons of the auditory nerve likely plays an important role in reproductive-related steroid-induced increases in peripheral auditory sensitivity in midshipman females as well (Forlano et al., 2005, 2006). Our previous studies also show improved hearing and visual capabilities in females as they approach spawning condition and ovulation that is associated with aromatase changes in the eye and saccule auditory endorgan (Butler et al., 2019; K. P. Maruska & Fernald, 2010c; Maruska et al., 2012), suggesting that similar modulatory mechanisms may exist in the cichlid.

Also consistent with that seen in other teleosts, the majority of aromatase-expression in the *A. burtoni* brain was found in radial glial cells that also co-express the glial marker GFAP. While this glial expression pattern seems to be the norm in teleosts, there is at least one exception where aromatase expression is found in ganglion cell bodies and fibers of the saccular auditory nerve in midshipman

(Forlano et al., 2005). Aromatase-expressing cells off the ventricular surface are also mentioned in other fishes (Menuet et al., 2003), but the cellular phenotype was not identified. We also observed several populations of aromatase-expressing cells located off the ventricular border, most notably in the preoptic area and diencephalic region near TPp and CP. These cell populations do not co-label with either GFAP or HuC/D, so their cellular identity is not known. It is possible they represent an intermediate phenotype as cells migrate from ventricular proliferation zones to their destinations and mature into neurons, or they may be glial cell subtypes that do not express GFAP.

6 | REPRODUCTIVE-STATE CHANGES IN BRAIN ESTROGEN SIGNALING AND FUNCTIONAL IMPLICATIONS

Female *A. burtoni* regularly cycle through gravid, mouth brooding, and recovering states, and each phase is associated with many cellular, morphological, physiological, and behavioral changes. Here we found higher mRNA levels of brain aromatase in all examined microdissected brain regions as females become gravid and approach spawning, which was also positively correlated with GSI and plasma estradiol

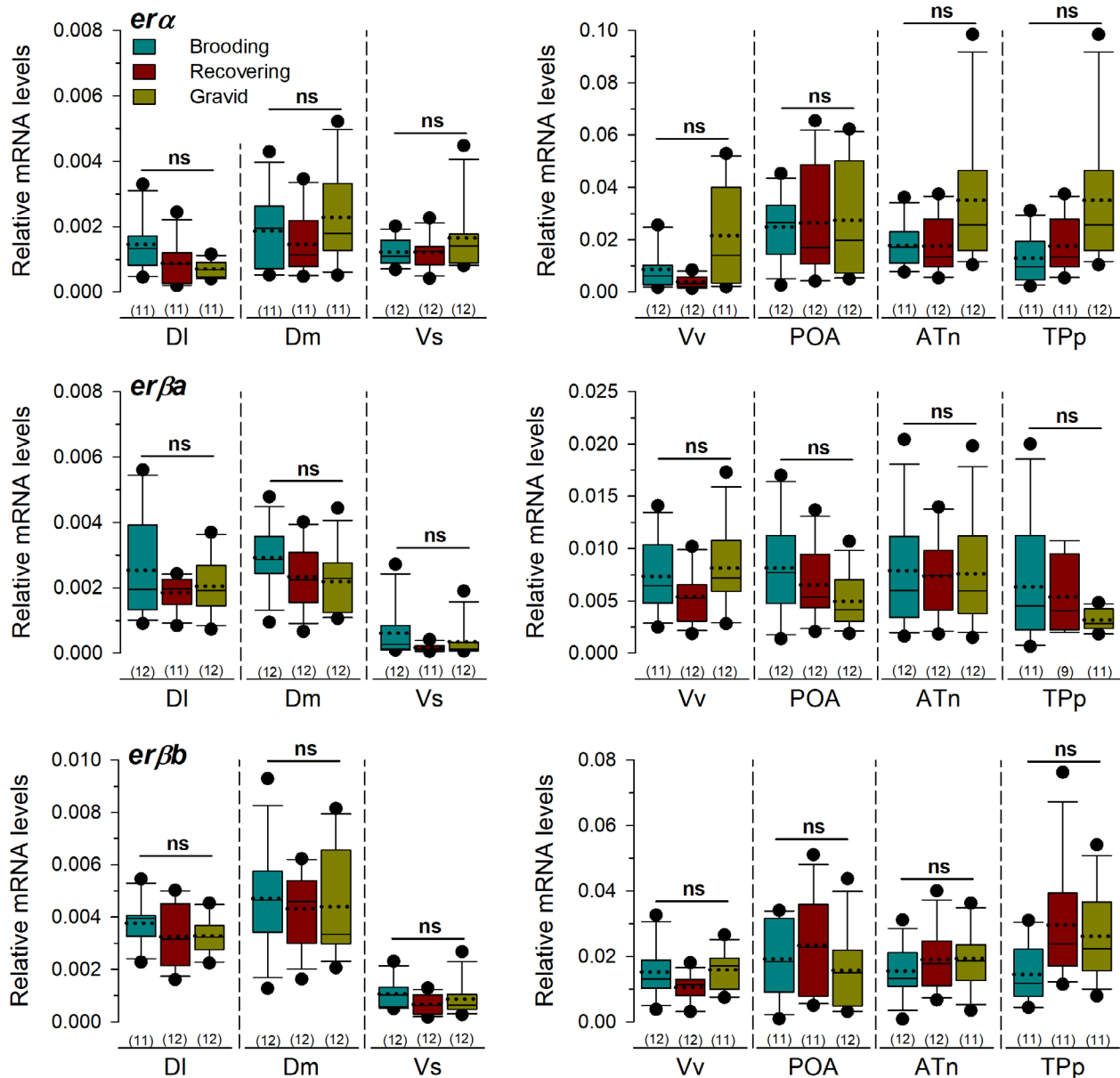


FIGURE 10 Expression of estrogen receptors in social decision centers of the brain does not differ across female reproductive state. mRNA levels of *era*, *erβa*, and *erβb* were not different among brooding, recovering, and gravid females for any microdissected brain region. Data are expressed relative to the geometric mean of the reference genes. ns, not significant at $p > .05$. See Figure 3 for box plot descriptions [Color figure can be viewed at wileyonlinelibrary.com]

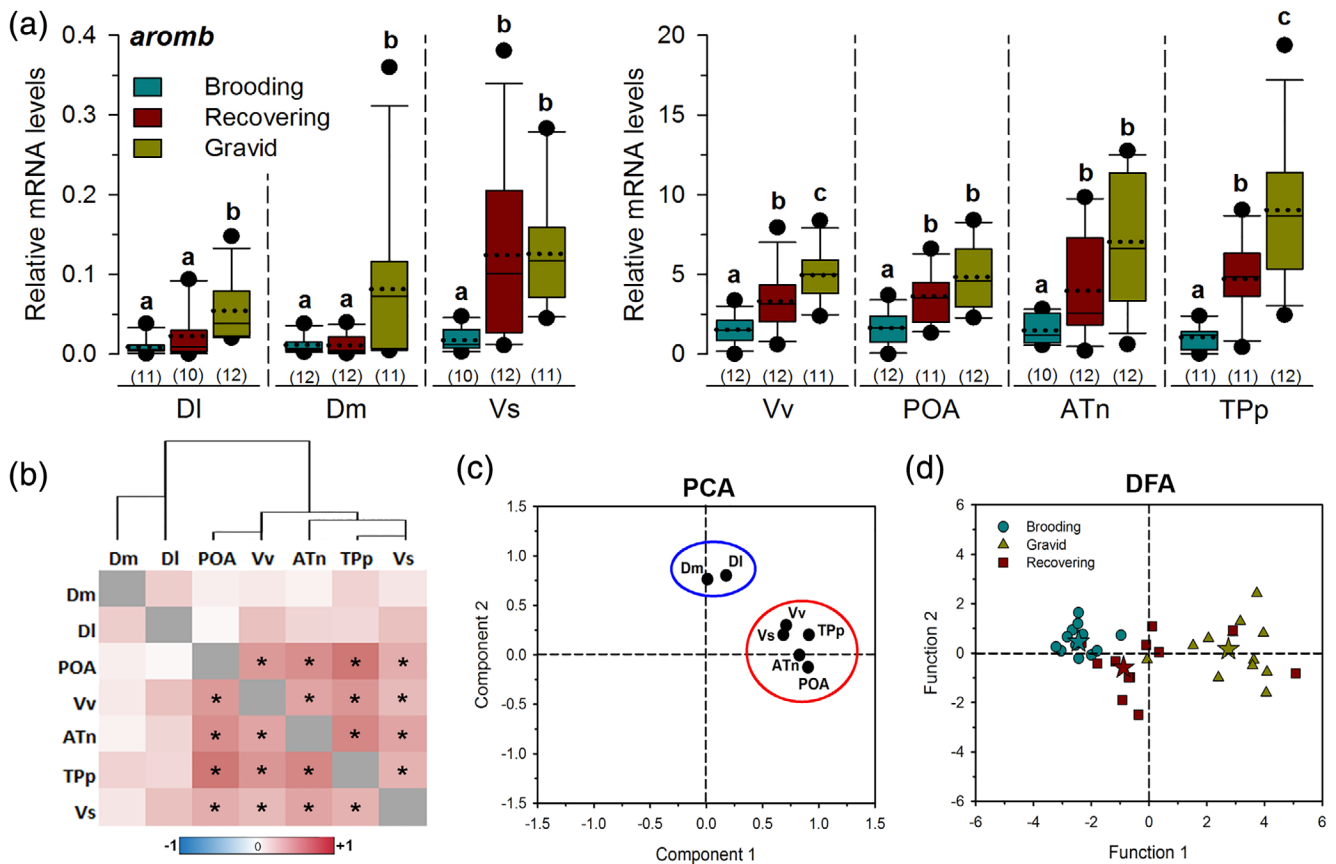


FIGURE 11 Aromatase expression in social decision centers of the brain varies across the female reproductive cycle. (a) Levels of aromatase mRNA are higher in females as they get closer to gravid spawning condition in all examined brain regions. Data are expressed relative to the geometric mean of the reference genes. See Figure 3 for box plot descriptions. Different letters indicate statistical differences at $p < .05$. (b) Hierarchical clustering and Pearson correlations (displayed as a heat map) were used to group brain regions based on *aromb* expression. Two different clusters were identified based on co-expression of aromatase: One with DI and Dm, and another in which POA, Vv, ATn, Tpp, and Vs were all significantly positively correlated with each other. R-values are represented by a color scale with red as positive and blue as negative correlations. Cells with an asterisk (*) indicate significant correlations. (c) Principal component analysis (PCA) revealed the identical two separate networks (DI and Dm group together, blue circle; POA, Vv, ATn, Tpp, and Vs group together, red circle). (d) Discriminant function analysis (DFA) correctly classified females into their respective groups based on aromatase expression alone. Gravid and brooding females clearly separate along function 1, while recovering females lie in the middle and overlap somewhat with both. Dots (brooding), squares (recovering), and triangles (gravid) represent individual fish, and group centroids are indicated by a star [Color figure can be viewed at wileyonlinelibrary.com]

TABLE 2 Post hoc p -values for GLM comparisons of *aromb* transcript levels in microdissected brain nuclei across female reproductive states

Region	Gr-re	Gr-Br	Br-re
DI	.015	.004	.535
Dm	.029	.049	.827
Vs	.136	.001	.047
Vv	.007	<.001	.045
POA	.152	.001	.024
ATn	.187	.001	.043
TPp	.006	<.001	.033
TS	<.001	<.001	.867
Te	<.001	<.001	.653

Note: Bold indicates significance at $p < .05$.
Abbreviations: Br, brooding; Gr, gravid; re, recovering.

levels. Aromatase activity is considered a good indicator of estrogen synthesis, and measuring aromatase mRNA levels with qPCR can reliably predict the quantity of functional protein (Sawyer, Gerstner, & Callard, 2006). Brain aromatase levels or activity, particularly in the preoptic area and hypothalamus, also vary across the female reproductive cycle in seasonally-breeding teleosts and correlate with ovarian status and circulating steroid levels. For example, brain aromatase activity peaked during the breeding season in female goldfish (Pasmanik & Callard, 1988) and European sea bass (Gonzalez & Piferrer, 2003), and during the prenesting period in plainfin midshipman (Forlano & Bass, 2005). The positive correlation between circulating estradiol and aromatase is not surprising because the brain aromatase gene contains a well-conserved ERE in its promoter, initiating a positive autoregulatory feedback loop (Diotel et al., 2010). In fishes, there is also evidence that the aromatase promoter is sensitive to estradiol only in specific cell contexts, and the ERE is necessary but

not sufficient for estrogenic activation in glial cells (Dietel et al., 2010). Further, aromatase mRNA levels in many brain regions were positively correlated with circulating 11-KT levels in the cichlid, and there is evidence across vertebrates that androgens can also regulate aromatase expression (Balthazart & Ball, 1998; Gelinas, Pitoc, & Callard, 1998; Resko, Pereyra-Martinez, Stadelman, & Roselli, 2000). In birds and mammals, aromatase activity can also be rapidly modulated by post-translational modifications like phosphorylation

(Balthazart et al., 2009). Thus, there are many complex mechanisms by which local estrogen influence can occur in the brain, and further studies are needed to examine the reproductive-state regulation of aromatase activity in the fish brain.

The ability of the brain to synthesize biologically functional levels of estrogens is a conserved characteristic of vertebrates, and the highest potential for neuroestrogen production is found in teleost fishes, which represent the largest (>30,000 species) and most diverse vertebrate group. The reason for high neuroestrogen production in the fish brain may be related to the extraordinary capacity of the adult fish central nervous system for neuroplasticity, regeneration, and neurogenesis. These processes may be needed for homeostatic maintenance or remodeling of neural circuitry in the female *A. burtoni* brain to control physiological aspects of ovary function and energetics, as well as sensory perception and behaviors related to mate choice, spawning, and maternal care, all of which change dramatically across the reproductive cycle. In goldfish, seasonal variations in brain aromatase are also associated with changes in levels of markers involved in neuronal growth and plasticity (e.g., β -actin, β -tubulin, and ribosomal RNAs; Gelinas et al., 1998), supporting a role in neural circuit remodeling to support reproductive-state specific activities. Higher aromatase could also be related to cell proliferation or changes in the cell life cycle, as shown in the female medaka tectum (Takeuchi & Okubo, 2013), especially given the remarkable overlap between aromatase-expressing cells and cell proliferation zones in the brain of *A. burtoni* (K. P. Maruska, Carpenter, et al., 2012) and other teleosts

TABLE 3 Pearson correlation coefficients and *p*-values of correlations between *aromb* levels in microdissected brain nuclei and gonadosomatic index (GSI) and circulating sex-steroid hormone levels

Region	GSI		E2		11KT	
	<i>r</i>	<i>p</i>	<i>r</i>	<i>p</i>	<i>r</i>	<i>p</i>
DI	.59	<.001	.44	.014	.53	.002
Dm	.52	<.001	.40	.031	.25	.144
Vs	.25	.159	.41	.020	.22	.224
Vv	.58	<.001	.70	<.001	.50	.003
POA	.54	<.001	.68	<.001	.32	.066
ATn	.49	.004	.76	<.001	.61	<.001
TPp	.64	<.001	.82	<.001	.50	.003
TS	.71	<.001	.42	.015	.53	.001
Te	.69	<.001	.48	.006	.34	.060

Note: Bold indicates significance at *p* < .05.

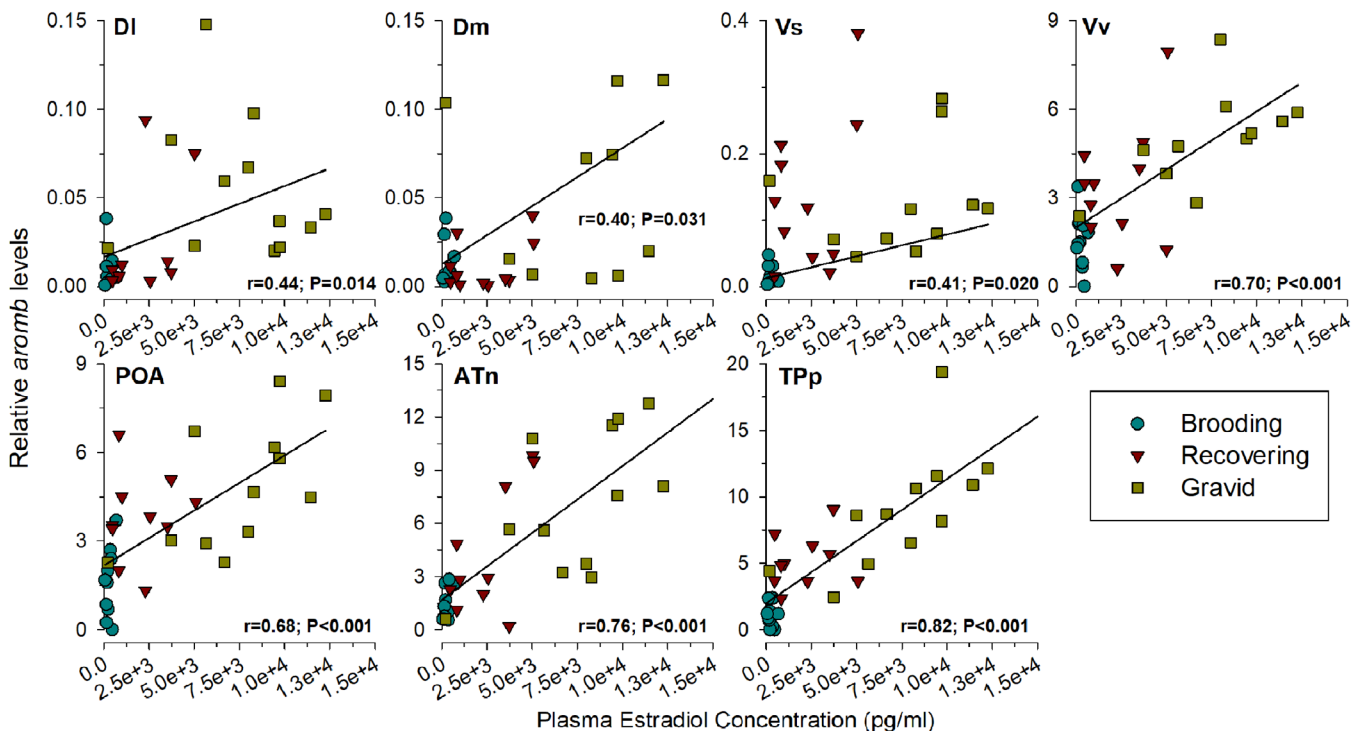


FIGURE 12 *Aromb* expression in the brain is positively correlated with circulating estradiol levels in female *A. burtoni*. *Aromb* mRNA levels are positively correlated with plasma estradiol concentrations in all brain regions. Each point represents an individual fish of brooding (cyan circles), recovering (red inverted triangles), and gravid (yellow squares) condition. Pearson correlation coefficients (*r*) and *p*-values for all fish together are shown on individual graphs of each microdissected brain region [Color figure can be viewed at wileyonlinelibrary.com]

(Dunlap, Silva, & Chung, 2011; Ekstrom, Johnsson, & Ohlin, 2001; Kuroyanagi et al., 2010; Zupanc, 2008). The estrogen-driven autoregulatory positive feedback loop (via estrogen action on EREs in promotor of *cyp19a1b* gene) in the brain may also amplify and prolong brain aromatase expression and activity, thereby elevating localized estrogen synthesis to sub-serve neural plasticity and processing.

Higher aromatase expression in the brain of gravid females may help mediate various social behaviors. Gravid females need to choose a male based on his courtship displays and territory, and then perform affiliative and spawning behaviors. Thus, local estrogen synthesis may mediate these decisions and resultant behaviors. Estrogen modulation of female sexual behaviors is common in fishes and other taxa (Balthazart et al., 2006; Munakata & Kobayashi, 2010). Gravid female *A. burtoni* can also show aggression towards other females (Field & Maruska, 2017; Renn, Fraser, Aubin-Horth, Trainor, & Hofmann, 2012), possibly related to mate competition. Given that aromatase and estrogens mediate aggressive behaviors in male *A. burtoni* (Huffman et al., 2013; O'Connell & Hofmann, 2012b) and other fishes (Black, Balthazart, Baillien, & Grober, 2005; Goncalves et al., 2009), it is possible that high brain aromatase in gravid females also helps modulate aggression. Another possibility is that high brain aromatase levels in gravid females may help prepare the brain for the upcoming mouth brooding phase, which is associated with an energetic consumption and starvation period along with brood care. Mouth brooding females sampled here about half way through their brood period showed low brain aromatase levels compared to the gravid state, but how rapidly they change after the onset of brooding requires further study. To our knowledge, no other study examined brain aromatase variations in a mouth brooding fish that deals with trade-offs between feeding/energetics, reproduction, and parental care, so additional comparative studies are needed to provide insight on its potential role in these processes. Interestingly, a recent study also demonstrated an estradiol-dependent regulation of stress effects mediated by astrocytic glial cells in the brain of females but not males (Bollinger, Salinas, Fender, Sengelaub, & Wellman, 2019), raising the possibility of stress-related functions associated with mating and subsequent mouth brooding in *A. burtoni*. Nevertheless, it is possible that sexual, aggressive, and other behaviors such as feeding, brood care, and stress coping in female *A. burtoni* are regulated by aromatase and estrogenic signaling in the brain.

Our PCA and hierarchical clustering analyses of aromatase levels across brain regions also revealed a pallial cluster of Dm and DI that was distinct from a second cluster that included the subpallial and diencephalic nuclei (Vv, Vs, POA, ATn, and TPp). While this may be explained by the difference in distribution and abundance of aromatase-expressing cells between these areas (e.g., primarily along the midline ventricle surfaces in the subpallial and diencephalic regions vs. the ventricle borders along the outer surface of the pallium) or some other unknown factors, it may also reflect distinct functional co-expression networks. In fact, our DFA analysis correctly classified most females (86%) into gravid, brooding, or recovering states based solely on aromatase expression levels in the brain, but was unable to do the same with estrogen receptor expression. All of these brain regions are

implicated in various social behaviors such as aggression, reproduction, parental care, and communication across vertebrate taxa (Goodson, 2005; O'Connell & Hofmann, 2011, 2012a), so local estrogen synthesis may help regulate these behaviors that change across the female reproductive cycle. We saw a similar pattern of higher aromatase expression in gravid females in all microdissected brain regions examined here, so it is likely that the entire brain experiences up-regulation of aromatase and increased estrogen synthesis as females undergo ovarian recrudescence. High aromatase expression in gravid females may also reduce the availability of active androgens in the brain to promote female-relevant behaviors. The localization of aromatase in radial glial cells and their processes that extend into the cellular and neuropil areas of many socially-relevant brain nuclei suggests that locally synthesized estrogens can modulate very specific neural circuits on both short-term (rapid, nongenomic) and long-term (genomic) time-scales. These regions all express estrogen receptors, but little is known about the functional implications of local estrogen production in specific nuclei of the fish brain.

In contrast to aromatase, we found that mRNA levels of estrogen receptors (*era*, *erβa*, *erβb*, and *gper* in POA) in the same brain regions did not vary across the female reproductive cycle and were not well correlated with either GSI or circulating steroids. While all of the examined regions contain measurable levels of ER mRNAs in female *A. burtoni*, and in situ hybridization confirms they are expressed (unpublished observations), they do not fluctuate with the reproductive cycle. This is not surprising, as studies in other teleosts show that ERs in the brain are often not influenced by sex-steroids (G. V. Callard et al., 2001). Changes in receptor levels may not be necessary to modify local circuits if levels are already sufficient, and locally raising the concentration of available estradiol via aromatization would enhance the number of receptors occupied and strengthen or amplify the response. Further, it is also possible that higher estradiol levels are needed to activate the membrane estrogen receptors like *gper* that are typically expressed in much lower levels than the nuclear receptors (also observed here in female *A. burtoni* POA). In fact, rapid nongenomic actions of estrogens are typically observed only after high dose administration of estradiol (Balthazart et al., 2006; Cornil, Ball, & Balthazart, 2006; Herbison, 2009). Thus, it may be that local estrogens produced in the female brain are necessary for any nongenomic rapid changes associated with courtship, ovulation, and spawning-related behaviors including sensory perception.

7 | COMPARISONS WITH MALES

Several previous studies in *A. burtoni* examined the role of estrogen signaling in males, providing relevant information for sex comparisons in this species. Male *A. burtoni* exist in a dominance hierarchy in which more dominant individuals are territorial, colorful, and reproductively active, while more subordinate males are nonterritorial, have drab coloration similar to females, and are reproductively suppressed (reviewed in (Fernald & Maruska, 2012; K. P. Maruska & Fernald, 2018, 2014). Male *A. burtoni* have high levels of circulating

estradiol, with levels in dominant males often greater than that seen in females (K. P. Maruska & Fernald, 2010b), and a recent study showed that levels of aromatase (*cyp19a1b*) are higher in the testis than both the brain and ovary (Bohne, Heule, Boileau, & Salzburger, 2013). Pharmacological manipulation of estrogen pathways in males shows that estradiol increases and is necessary for aggressive behavior (O'Connell & Hofmann, 2012b), and treatment of dominant males with the aromatase inhibitor fadrozole decreases aggressive but not reproductive behaviors (Huffman et al., 2013). While long-term (days to months) treatment of females with aromatase inhibitor causes male-like dominance behaviors and coloration over time (Goppert et al., 2016), the role of estrogen signaling in mediating more rapid behaviors in *A. burtoni* females remains unexplored.

Using the identical technique of measuring estrogen signaling-related mRNA levels in microdissected brain regions used here (aromatase and estrogen receptors), a previous study of *A. burtoni* males showed that dominant reproductively active males had higher aromatase levels in several regions (Vv, VTn, Ce, and pituitary), but not in many others (Dm, DI, Vs, POA, ATn; TPp was not examined) (K. P. Maruska, Zhang, et al., 2013). An ISH study also detected no male status differences in many socially-relevant brain areas (e.g., Vv, Vd, pPOA, ATn, TPp), but revealed that subordinate males have higher aromatase expression in specific regions of the preoptic area (mPOA and gPOA) compared to dominant males (Huffman et al., 2013). Thus, aromatase expression appears up-regulated throughout the brain in reproductive female *A. burtoni*, while reproductive-state changes in males only occurs in specific nuclei. Further, in contrast to that seen here in females, some differences between dominant and subordinate males in estrogen receptor mRNA levels (*era*, *er β a*, *er β b*) were revealed in some microdissected brain regions of males of different social status (K. P. Maruska, Zhang, et al., 2013). Collectively, these differences between males and females suggest there may be sex differences in the mechanisms regulating brain estrogenic signaling. There are often sex differences in brain aromatase levels (and presumably neuroestrogens) of other species, but whether levels are higher in males or females seems to depend on the species (i.e., most birds and mammals, and some teleosts show higher levels in males, while some other fishes show higher levels in females) (Gonzalez & Piferrer, 2003; Roselli, 1991; Schumacher & Balthazart, 1986). It is not possible to directly compare the mRNA levels measured by qPCR here to those previously measured in males because of different reference genes and animal sizes, but several other studies in teleosts detect intra and/or intersex differences in brain aromatase levels or distribution patterns (Forlano & Bass, 2005; Okubo et al., 2011; Schlinger, Greco, & Bass, 1999; Strobl-Mazzulla et al., 2008), while in other species, no obvious sex differences are observed (Goto-Kazeto et al., 2004; Shaw & Krahe, 2018). A study in the medaka also demonstrated that the female-biased aromatase expression in the brain is related to activational rather than organizational effects of estradiol (Okubo et al., 2011). Collectively, these results highlight the importance of examining inter and intrasexual differences in both males and females within a single species, but future work is needed to determine the regulatory mechanisms and biological significance of these sex differences in diverse taxa.

8 | CONCLUSIONS

The African cichlid fish *A. burtoni* is a valuable system to examine the role of neurosteroids in social behaviors, reproductive physiology, and communication. The majority of research in *A. burtoni* is focused on males, but it is clear that the brain and neural circuits differ between the sexes across vertebrates and we cannot extrapolate findings in males to females even within the same species. We focused here on *A. burtoni* females to provide insights on the importance of estrogen signaling in the brain in a species that cycles through gravid, mouth brooding, and recovering states that are associated with distinct changes in reproductive physiology, feeding and energetic status, social behaviors including maternal care, and sensory perception. Our results show greater mRNA levels of the enzyme aromatase, which catalyzes conversion of testosterone to estrogens, in microdissected socially-relevant and sensory brain regions in gravid females with large oocytes and high circulating sex-steroid levels. The mRNA levels of estrogen receptors, however, did not vary with female reproductive state. We also localized aromatase-expressing cells throughout the cichlid brain, and demonstrate expression in radial glial cells along ventricle borders from the forebrain to the hindbrain. While the expression pattern is overall similar to other teleosts, there are some distinct differences among teleost species that may have functional implications and deserve future attention. Our ISH also confirmed greater aromatase staining in gravid compared to mouth brooding females. The high aromatase expression in the brain of adult teleosts, and its relatively conserved expression patterns in the brain suggest that brain-derived estrogen synthesis is important in this speciose vertebrate group. The function of localized estrogenic signaling in the teleost brain is relatively unexplored however, and future work should examine how estrogen synthesis might modulate neural function on single neuron, circuit, and behavioral levels before we can fully understand the implications of any reproductive-state changes in the brain.

ACKNOWLEDGMENTS

We thank members of the Maruska lab for fish maintenance and experimental assistance. Funding was provided by the National Science Foundation (IOS-1456004 and IOS-1456558 to K. P. M.). J. M. B. was supported by a Louisiana Board of Regents Fellowship and an NSF Graduate Research Fellowship (1247192). G.T. was supported by the Louisiana Biomedical Research Network (LBRN; NIH P20 GM103424-17) summer program at LSU.

CONFLICT OF INTEREST

The authors have no known or potential conflicts of interest.

AUTHOR CONTRIBUTIONS

All authors had full access to the data, take responsibility for the integrity of the data analysis, and approved the final manuscript. Julie M. Butler collected animals and performed steroid hormone assays. Julie M. Butler, Chase Anselmo, and Ganga Tandukar performed ISH and double ISH-IHC. Karen P. Maruska performed microdissections and qPCR. Karen P. Maruska, Julie M. Butler, Chase Anselmo, and

Ganga Tandukar analyzed and interpreted the data. Karen P. Maruska wrote the initial manuscript draft and all authors edited the article into its final version. Karen P. Maruska provided equipment, resources, and funding.

DATA AVAILABILITY STATEMENT

The data that support the findings of this study are available from the corresponding author upon reasonable request.

ORCID

Karen P. Maruska  <https://orcid.org/0000-0003-2425-872X>

Julie M. Butler  <https://orcid.org/0000-0002-7400-8780>

REFERENCES

- Ampatzis, K., & Dermon, C. R. (2011). Regional distribution and cellular localization of β_2 -adrenoceptors in the adult zebrafish brain (*Danio rerio*). *The Journal of Comparative Neurology*, 518(9), 1418–1441. <https://doi.org/10.1002/cne.22278>
- Balthazart, J., & Ball, G. F. (1998). New insights into the regulation and function of brain estrogen synthase (aromatase). *Trends in Neurosciences*, 21(6), 243–249.
- Balthazart, J., Cornil, C. A., Taziaux, M., Charlier, T. D., Baillien, M., & Ball, G. F. (2006). Rapid changes in production and behavioral action of estrogens. *Neuroscience*, 138(3), 783–791. <https://doi.org/10.1016/j.neuroscience.2005.06.016>
- Balthazart, J., Taziaux, M., Holloway, K., Ball, G. F., & Cornil, C. A. (2009). Behavioral effects of brain-derived estrogens in birds. *Annals of the New York Academy of Sciences*, 1163, 31–48. <https://doi.org/10.1111/j.1749-6632.2008.03637.x>
- Barami, K., Iversen, K., Furneaux, H., & Goldman, S. A. (1995). Hu protein as an early marker of neuronal phenotypic differentiation by subependymal zone cells of the adult songbird forebrain. *Journal of Neurobiology*, 28(1), 82–101. <https://doi.org/10.1002/neu.480280108>
- Black, M. P., Balthazart, J., Baillien, M., & Grober, M. S. (2005). Socially induced and rapid increases in aggression are inversely related to brain aromatase activity in a sex-changing fish, *Lythrypnus dalli*. *Proceedings of the Royal Society B: Biological Sciences*, 272(1579), 2435–2440. <https://doi.org/10.1098/rspb.2005.3210>
- Bohne, A., Heule, C., Boileau, N., & Salzburger, W. (2013). Expression and sequence evolution of aromatase cyp19a1 and other sexual development genes in east African cichlid fishes. *Molecular Biology and Evolution*, 30(10), 2268–2285. <https://doi.org/10.1093/molbev/mst124>
- Bollinger, J. L., Salinas, I., Fender, E., Sengelaub, D. R., & Wellman, C. L. (2019). Gonadal hormones differentially regulate sex-specific stress effects on glia in the medial prefrontal cortex. *Journal of Neuroendocrinology*, 31, e12762. <https://doi.org/10.1111/jne.12762>
- Burmeister, S. S., Kailasanath, V., & Fernald, R. D. (2007). Social dominance regulates androgen and estrogen receptor gene expression. *Hormones and Behavior*, 51(1), 164–170. <https://doi.org/10.1016/j.yhbeh.2006.09.008>
- Burmeister, S. S., Munshi, R. G., & Fernald, R. D. (2009). Cytoarchitecture of a cichlid fish telencephalon. *Brain, Behavior and Evolution*, 74(2), 110–120. <https://doi.org/10.1159/000235613>
- Butler, J. M., & Maruska, K. P. (2016). The mechanosensory lateral line system mediates activation of socially relevant brain regions during territorial interactions. *Frontiers in Behavioral Neuroscience*, 10, 93.
- Butler, J. M., Whitlow, S. M., Rogers, L. S., Putland, R. L., Mensinger, A. F., & Maruska, K. P. (2019). Reproductive state-dependent plasticity in the visual system of an African cichlid fish. *Hormones and Behavior*, 114, 104539.
- Callard, G., Schlinger, B., & Pasmanik, M. (1990). Nonmammalian vertebrate models in studies of brain-steroid interactions. *The Journal of Experimental Zoology. Supplement*, 4, 6–16.
- Callard, G. V., Tchoudakova, A. V., Kishida, M., & Wood, E. (2001). Differential tissue distribution, developmental programming, estrogen regulation and promoter characteristics of cyp19 genes in teleost fish. *The Journal of Steroid Biochemistry and Molecular Biology*, 79(1–5), 305–314.
- Cornil, C. A. (2018). On the role of brain aromatase in females: Why are estrogens produced locally when they are available systemically? *Journal of Comparative Physiology. A, Neuroethology, Sensory, Neural, and Behavioral Physiology*, 204(1), 31–49. <https://doi.org/10.1007/s00359-017-1224-2>
- Cornil, C. A., Ball, G. F., & Balthazart, J. (2006). Functional significance of the rapid regulation of brain estrogen action: Where do the estrogens come from? *Brain Research*, 1126(1), 2–26. <https://doi.org/10.1016/j.brainres.2006.07.098>
- Cornil, C. A., Dalla, C., Papadopoulou-Daifoti, Z., Baillien, M., & Balthazart, J. (2006). Estradiol rapidly activates male sexual behavior and affects brain monoamine levels in the quail brain. *Behavioural Brain Research*, 166(1), 110–123. <https://doi.org/10.1016/j.bbr.2005.07.017>
- Cornil, C. A., & de Bournonville, C. (2018). Dual action of neuro-estrogens in the regulation of male sexual behavior. *General and Comparative Endocrinology*, 256, 57–62. <https://doi.org/10.1016/j.ygcen.2017.05.002>
- Cross, E., & Roselli, C. E. (1999). 17beta-estradiol rapidly facilitates chemoinvestigation and mounting in castrated male rats. *The American Journal of Physiology*, 276(5), R1346–R1350. <https://doi.org/10.1152/ajpregu.1999.276.5.R1346>
- Diotel, N., Do Rego, J. L., Anglade, I., Vaillant, C., Pellegrini, E., Gueguen, M. M., ... Kah, O. (2011). Activity and expression of steroidogenic enzymes in the brain of adult zebrafish. *The European Journal of Neuroscience*, 34(1), 45–56. <https://doi.org/10.1111/j.1460-9568.2011.07731.x>
- Diotel, N., Le Page, Y., Mouriec, K., Tong, S. K., Pellegrini, E., Vaillant, C., ... Kah, O. (2010). Aromatase in the brain of teleost fish: Expression, regulation and putative functions. *Frontiers in Neuroendocrinology*, 31(2), 172–192. <https://doi.org/10.1016/j.yfrne.2010.01.003>
- Dunlap, K. D., Silva, A. C., & Chung, M. (2011). Environmental complexity, seasonality and brain cell proliferation in a weakly electric fish, *Brachyhypopomus gauderio*. *Journal of Experimental Biology*, 214(Pt 5), 794–805. <https://doi.org/10.1242/jeb.051037>
- Ekstrom, P., Johnsson, C. M., & Ohlin, L. M. (2001). Ventricular proliferation zones in the brain of an adult teleost fish and their relation to neuromeres and migration (secondary matrix) zones. *The Journal of Comparative Neurology*, 436(1), 92–110.
- Elliott, S. B., Harvey-Girard, E., Giassi, A. C., & Maler, L. (2017). Hippocampal-like circuitry in the pallium of an electric fish: Possible substrates for recursive pattern separation and completion. *The Journal of Comparative Neurology*, 525(1), 8–46. <https://doi.org/10.1002/cne.24060>
- Fernald, R. D., & Maruska, K. P. (2012). Social information changes the brain. *Proceedings of the National Academy of Sciences of the United States of America*, 109(Suppl. 2), 17194–17199. <https://doi.org/10.1073/pnas.1202552109>
- Fernald, R. D., & Shelton, L. C. (1985). The organization of the diencephalon and the preteum in the cichlid fish, *Haplochromis burtoni*. *The Journal of Comparative Neurology*, 238(2), 202–217.
- Field, K. F., & Maruska, K. P. (2017). Context-dependent chemosensory signaling, aggression, and neural activation patterns in gravid female African cichlid fish. *The Journal of Experimental Biology*, 220, 4689–4702.

- Forlano, P. M., & Bass, A. H. (2005). Seasonal plasticity of brain aromatase mRNA expression in glia: Divergence across sex and vocal phenotypes. *Journal of Neurobiology*, 65(1), 37–49.
- Forlano, P. M., Deitcher, D. L., & Bass, A. H. (2005). Distribution of estrogen receptor alpha mRNA in the brain and inner ear of a vocal fish with comparisons to sites of aromatase expression. *The Journal of Comparative Neurology*, 483(1), 91–113.
- Forlano, P. M., Deitcher, D. L., Myers, D. A., & Bass, A. H. (2001). Anatomical distribution and cellular basis for high levels of aromatase activity in the brain of teleost fish: Aromatase enzyme an mRNA expression identify glia as source. *Journal of Neuroscience*, 21(22), 8943–8955.
- Forlano, P. M., Schlinger, B. A., & Bass, A. H. (2006). Brain aromatase: New lessons from non-mammalian model systems. *Frontiers in Neuroendocrinology*, 27(3), 247–274.
- Gelinas, D., Pitoc, G. A., & Callard, G. V. (1998). Isolation of a goldfish brain cytochrome P450 aromatase cDNA: mRNA expression during the seasonal cycle and after steroid treatment. *Molecular and Cellular Endocrinology*, 138(1–2), 81–93.
- Goncalves, D., Saraiva, J., Teles, M., Teodosio, R., Canario, A. V., & Oliveira, R. F. (2009). Brain aromatase mRNA expression in two populations of the peacock blenny *Salaria pavo* with divergent mating systems. *Hormones and Behavior*, 57(2), 155–161. <https://doi.org/10.1016/j.yhbeh.2009.10.007>
- Gonzalez, A., & Piferrer, F. (2003). Aromatase activity in the European sea bass (*Dicentrarchus labrax* L.) brain. Distribution and changes in relation to age, sex, and the annual reproductive cycle. *General and Comparative Endocrinology*, 132(2), 223–230.
- Goodson, J. L. (2005). The vertebrate social behavior network: Evolutionary themes and variations. *Hormones and Behavior*, 48(1), 11–22.
- Goodson, J. L., & Kingsbury, M. A. (2013). What's in a name? Considerations of homologies and nomenclature for vertebrate social behavior networks. *Hormones and Behavior*, 64(1), 103–112. <https://doi.org/10.1016/j.yhbeh.2013.05.006>
- Goppert, C., Harris, R. M., Theis, A., Boila, A., Hohl, S., Ruegg, A., ... Bohne, A. (2016). Inhibition of aromatase induces partial sex change in a cichlid fish: Distinct functions for sex steroids in brains and gonads. *Sexual Development*, 10(2), 97–110. <https://doi.org/10.1159/000445463>
- Goto-Kazeto, R., Kight, K. E., Zohar, Y., Place, A. R., & Trant, J. M. (2004). Localization and expression of aromatase mRNA in adult zebrafish. *General and Comparative Endocrinology*, 139(1), 72–84. <https://doi.org/10.1016/j.ygcen.2004.07.003>
- Grone, B. P., & Maruska, K. P. (2015). A second corticotropin-releasing hormone gene (CRH2) is conserved across vertebrate classes and expressed in the hindbrain of a basal neopterygian fish, the spotted gar (*Lepisosteus oculatus*). *Journal of Comparative Neurology*, 523, 1125–1143.
- Gunther, A. (1894). Descriptions of the reptiles and fishes collected by Mr. E. Coode-hore on Lake Tanganyika. *Proceedings of the Zoological Society of London*, 628–632.
- Herbison, A. E. (2009). Rapid actions of oestrogen on gonadotropin-releasing hormone neurons; from fantasy to physiology? *The Journal of Physiology*, 587(Pt. 21), 5025–5030. <https://doi.org/10.1113/jphysiol.2009.179838>
- Huffman, L. S., O'Connell, L. A., & Hofmann, H. A. (2013). Aromatase regulates aggression in the African cichlid fish *Astatotilapia burtoni*. *Physiology & Behavior*, 112–113, 77–83. <https://doi.org/10.1016/j.physbeh.2013.02.004>
- Jeng, S., Yueh, W., Pen, Y., Gueguen, M., Pasquier, J., Dufour, S., ... Kah, O. (2012). Expression of aromatase in radial glial cells in the brain of the Japanese eel provides insights into the evolution of the *cyp19a* gene in Actinopterygians. *PLoS One*, 7(9), e44750.
- Kayo, D., Zempo, B., Tomihara, S., Oka, Y., & Kanda, S. (2019). Gene knockout analysis reveals essentiality of estrogen receptor beta1 (*Esr2a*) for female reproduction in medaka. *Scientific Reports*, 9(1), 8868. <https://doi.org/10.1038/s41598-019-45373-y>
- Kuroyanagi, Y., Okuyama, T., Suehiro, Y., Imada, H., Shimada, A., Naruse, K., ... Takeuchi, H. (2010). Proliferation zones in adult medaka (*Oryzias latipes*) brain. *Brain Research*, 1323, 33–40. <https://doi.org/10.1016/j.brainres.2010.01.045>
- Lai, Y. J., Yu, D., Zhang, J. H., & Chen, G. J. (2017). Cooperation of genomic and rapid nongenomic actions of estrogens in synaptic plasticity. *Molecular Neurobiology*, 54(6), 4113–4126. <https://doi.org/10.1007/s12035-016-9979-y>
- Luine, V., Serrano, P., & Frankfurt, M. (2018). Rapid effects on memory consolidation and spine morphology by estradiol in female and male rodents. *Hormones and Behavior*, 104, 111–118. <https://doi.org/10.1016/j.yhbeh.2018.04.007>
- Mangiamele, L. A., Gomez, J. R., Curtis, N. J., & Thompson, R. R. (2017). GPER/GPR30, a membrane estrogen receptor, is expressed in the brain and retina of a social fish (*Carassius auratus*) and colocalizes with isotocin. *The Journal of Comparative Neurology*, 525(2), 252–270. <https://doi.org/10.1002/cne.24056>
- Marsh, K. E., Creutz, L. M., Hawkins, M. B., & Godwin, J. (2006). Aromatase immunoreactivity in the bluehead wrasse brain, *Thalassoma bifasciatum*: Immunolocalization and co-regionalization with arginine vasotocin and tyrosine hydroxylase. *Brain Research*, 1126, 91–101.
- Marusich, M. F., Furneaux, H. M., Henion, P. D., & Weston, J. A. (1994). Hu neuronal proteins are expressed in proliferating neurogenic cells. *Journal of Neurobiology*, 25(2), 143–155. <https://doi.org/10.1002/neu.480250206>
- Maruska, K. P. (2015). Social transitions cause rapid behavioral and neuroendocrine changes. *Integrative and Comparative Biology*, 55, 294–306. <https://doi.org/10.1093/icb/icc/057>
- Maruska, K. P., Becker, L., Neboori, A., & Fernald, R. D. (2013). Social descent with territory loss causes rapid behavioral, endocrine, and transcriptional changes in the brain. *The Journal of Experimental Biology*, 216, 3656–3666. <https://doi.org/10.1242/jeb.088617>
- Maruska, K. P., Butler, J. M., Field, K. E., & Porter, D. T. (2017). Localization of glutamatergic, GABAergic, and cholinergic neurons in the brain of the African cichlid fish, *Astatotilapia burtoni*. *The Journal of Comparative Neurology*, 525(3), 610–638. <https://doi.org/10.1002/cne.24092>
- Maruska, K. P., Carpenter, R. E., & Fernald, R. D. (2012). Characterization of cell proliferation throughout the brain of the African cichlid fish *Astatotilapia burtoni* and its regulation by social status. *The Journal of Comparative Neurology*, 520(15), 3471–3491. <https://doi.org/10.1002/cne.23100>
- Maruska, K. P., & Fernald, R. D. (2010a). Reproductive status regulates expression of sex steroid and GnRH receptors in the olfactory bulb. *Behavioural Brain Research*, 213, 208–217. <https://doi.org/10.1016/j.bbr.2010.04.058>
- Maruska, K. P., & Fernald, R. D. (2010b). Steroid receptor expression in the fish inner ear varies with sex, social status, and reproductive state. *BMC Neuroscience*, 11, 58.
- Maruska, K. P., & Fernald, R. D. (2012). Contextual chemosensory urine signaling in an African cichlid fish. *The Journal of Experimental Biology*, 215, 68–74.
- Maruska, K. P., & Fernald, R. D. (2014). Social regulation of gene expression in the African cichlid fish *Astatotilapia burtoni*. In T. Canli (Ed.), *Handbook of molecular psychology* (pp. 52–78). New York, NY: Oxford University Press.
- Maruska, K. P., & Fernald, R. D. (2018). *Astatotilapia burtoni*: A model system for analyzing the neurobiology of behavior. *ACS Chemical Neuroscience*, 9, 1951–1962. <https://doi.org/10.1021/acscchemneuro.7b00496>
- Maruska, K. P., Ung, U. S., & Fernald, R. D. (2012). The African cichlid fish *Astatotilapia burtoni* uses acoustic communication for reproduction: Sound production, hearing, and behavioral significance. *PLoS One*, 7(5), e37612. <https://doi.org/10.1371/journal.pone.0037612>
- Maruska, K. P., Zhang, A., Neboori, A., & Fernald, R. D. (2013). Social opportunity causes rapid transcriptional changes in the social behavior

- network of the brain in an African cichlid fish. *Journal of Neuroendocrinology*, 25, 145–157.
- Maximino, C., Lima, M. G., Oliveira, K. R., Batista, E. D., & Herculano, A. M. (2012). "limbic associative" and "autonomic" amygdala in teleosts: A review of the evidence. *Journal of Chemical Neuroanatomy*, 48–49, 1–13. <https://doi.org/10.1016/j.jchemneu.2012.10.001>
- Menuet, A., Anglade, I., Le Guevel, R., Pellegrini, E., Pakdel, F., & Kah, O. (2003). Distribution of aromatase mRNA and protein in the brain and pituitary of female rainbow trout: Comparison with estrogen receptor alpha. *The Journal of Comparative Neurology*, 462(2), 180–193.
- Munakata, A., & Kobayashi, M. (2010). Endocrine control of sexual behavior in teleost fish. *General and Comparative Endocrinology*, 165(3), 456–468. <https://doi.org/10.1016/j.ygcen.2009.04.011>
- Munoz-Cueto, J. A., Sarasquete, C., Zohar, A. H., & Kah, O. (2001). *An atlas of the brain of the gilthead seabream (Sparus aurata)*. College Park: Maryland Sea Grant.
- Newman, S. W. (1999). The medial extended amygdala in male reproductive behavior. A node in the mammalian social behavior network. *Annals of the New York Academy of Sciences*, 877, 242–257.
- O'Connell, L. A., & Hofmann, H. A. (2011). The vertebrate mesolimbic reward system and social behavior network: A comparative synthesis. *The Journal of Comparative Neurology*, 519, 3599–3639. <https://doi.org/10.1002/cne.22735>
- O'Connell, L. A., & Hofmann, H. A. (2012a). Evolution of a vertebrate social decision-making network. *Science*, 336, 1154–1157.
- O'Connell, L. A., & Hofmann, H. A. (2012b). Social status predicts how sex steroid receptors regulate complex behavior across levels of biological organization. *Endocrinology*, 153(3), 1341–1351.
- Okubo, K., Takeuchi, A., Chaube, R., Paul-Prasanth, B., Kanda, S., Oka, Y., & Nagahama, Y. (2011). Sex differences in aromatase gene expression in the medaka brain. *Journal of Neuroendocrinology*, 23(5), 412–423. <https://doi.org/10.1111/j.1365-2826.2011.02120.x>
- Pasmanik, M., & Callard, G. V. (1985). Aromatase and 5(alpha)-reductase in the teleost brain, spinal cord, and pituitary gland. *General and Comparative Endocrinology*, 60, 244–251.
- Pasmanik, M., & Callard, G. V. (1988). Changes in brain aromatase and 5 alpha-reductase activities correlate significantly with seasonal reproductive cycles in goldfish (*Carassius auratus*). *Endocrinology*, 122(4), 1349–1356.
- Ponti, G., Farinetti, A., Marraudino, M., Panzica, G., & Gotti, S. (2018). Sex steroids and adult neurogenesis in the ventricular-subventricular zone. *Frontiers in Endocrinology (Lausanne)*, 9, 156. <https://doi.org/10.3389/fendo.2018.00156>
- Porter, D. T., Roberts, D., & Maruska, K. P. (2017). Distribution and female reproductive state differences in orexigenic and anorexigenic neurons in the brain of the african cichlid fish, *Astatotilapia burtoni*. *Journal of Comparative Neurology*, 525, 3126–3157.
- Remage-Healey, L., & Bass, A. H. (2006). From social behavior to neural circuitry: Steroid hormones rapidly modulate advertisement calling via a vocal pattern generator. *Hormones and Behavior*, 50(3), 432–441. <https://doi.org/10.1016/j.yhbeh.2006.05.007>
- Remage-Healey, L., & Bass, A. H. (2007). Plasticity in brain sexuality is revealed by the rapid actions of steroid hormones. *The Journal of Neuroscience*, 27(4), 1114–1122.
- Remage-Healey, L., Coleman, M. J., Oyama, R. K., & Schlinger, B. A. (2010). Brain estrogens rapidly strengthen auditory encoding and guide song preference in a songbird. *Proceedings of the National Academy of Sciences of the United States of America*, 107(8), 3852–3857. <https://doi.org/10.1073/pnas.0906572107>
- Remage-Healey, L., Jeon, S. D., & Joshi, N. R. (2013). Recent evidence for rapid synthesis and action of oestrogens during auditory processing in a songbird. *Journal of Neuroendocrinology*, 25(11), 1024–1031. <https://doi.org/10.1111/jne.12055>
- Remage-Healey, L., Maidment, N. T., & Schlinger, B. A. (2008). Fore-brain steroid levels fluctuate rapidly during social interactions. *Nature Neuroscience*, 11(11), 1327–1334. <https://doi.org/10.1038/nn.2200>
- Remage-Healey, L., Oyama, R. K., & Schlinger, B. A. (2009). Elevated aromatase activity in forebrain synaptic terminals during song. *Journal of Neuroendocrinology*, 21(3), 191–199. <https://doi.org/10.1111/j.1365-2826.2009.01820.x>
- Renn, S. C., Fraser, E. J., Aubin-Horth, N., Trainor, B. C., & Hofmann, H. A. (2012). Females of an African cichlid fish display male-typical social dominance behavior and elevated androgens in the absence of males. *Hormones and Behavior*, 61, 496–503.
- Resko, J. A., Pereyra-Martinez, A. C., Stadelman, H. L., & Roselli, C. E. (2000). Region-specific regulation of cytochrome P450 aromatase messenger ribonucleic acid by androgen in brains of male rhesus monkeys. *Biology of Reproduction*, 62(6), 1818–1822.
- Romero-Morales, L., Martinez-Torres, M., Cardenas, M., Alvarez, C., Carmona, A., Cedillo, B., & Luis, J. (2018). An increase in estradiol facilitates the onset of paternal behavior in the dwarf hamster (*Phodopus campbelli*). *Hormones and Behavior*, 99, 35–40. <https://doi.org/10.1016/j.yhbeh.2018.02.002>
- Roselli, C. E. (1991). Sex differences in androgen receptors and aromatase activity in microdissected regions of the rat brain. *Endocrinology*, 128(3), 1310–1316. <https://doi.org/10.1210/endo-128-3-1310>
- Sawyer, S. J., Gerstner, K. A., & Callard, G. V. (2006). Real-time PCR analysis of cytochrome P450 aromatase expression in zebrafish: Gene specific tissue distribution, sex differences, developmental programming, and estrogen regulation. *General and Comparative Endocrinology*, 147(2), 108–117. <https://doi.org/10.1016/j.ygcen.2005.12.010>
- Schlinger, B. A., & Callard, G. V. (1989). Aromatase activity in quail brain: Correlation with aggressiveness. *Endocrinology*, 124(1), 437–443. <https://doi.org/10.1210/endo-124-1-437>
- Schlinger, B. A., Greco, C., & Bass, A. H. (1999). Aromatase activity in hind-brain vocal control region: Divergence between "singing" and "sneaking" males. *Proceedings of the Royal Society B: Biological Sciences*, 266, 131–136.
- Schumacher, M., & Balthazart, J. (1986). Testosterone-induced brain aromatase is sexually dimorphic. *Brain Research*, 370(2), 285–293. [https://doi.org/10.1016/0006-8993\(86\)90483-x](https://doi.org/10.1016/0006-8993(86)90483-x)
- Shaw, K. (2018). Aromatase expression and function in the brain and behavior: A comparison across communication systems in teleosts. *Journal of Chemical Neuroanatomy*, 94, 139–153. <https://doi.org/10.1016/j.jchemneu.2018.10.004>
- Shaw, K., & Krahe, R. (2018). Pattern of aromatase mRNA expression in the brain of a weakly electric fish, *Apteronotus leptorhynchus*. *Journal of Chemical Neuroanatomy*, 90, 70–79. <https://doi.org/10.1016/j.jchemneu.2017.12.009>
- Sheppard, P. A. S., Choleris, E., & Galea, L. A. M. (2019). Structural plasticity of the hippocampus in response to estrogens in female rodents. *Molecular Brain*, 12(1), 22. <https://doi.org/10.1186/s13041-019-0442-7>
- Strobl-Mazzulla, P. H., Lethimonier, C., Gueguen, M. M., Karube, M., Fernandino, J. I., Yoshizaki, G., ... Somoza, G. M. (2008). Brain aromatase (Cyp19A2) and estrogen receptors, in larvae and adult pejerrey fish *Odontesthes bonariensis*: Neuroanatomical and functional relations. *General and Comparative Endocrinology*, 158(2), 191–201. <https://doi.org/10.1016/j.ygcen.2008.07.006>
- Strobl-Mazzulla, P. H., Moncaut, N. P., Lopez, G. C., Miranda, L. A., Canario, A. V., & Somoza, G. M. (2005). Brain aromatase from pejerrey fish (*Odontesthes bonariensis*): cDNA cloning, tissue expression, and immunohistochemical localization. *General and Comparative Endocrinology*, 143(1), 21–32. <https://doi.org/10.1016/j.ygcen.2005.02.026>
- Takeuchi, A., & Okubo, K. (2013). Post-proliferative immature radial glial cells female-specifically express aromatase in the medaka optic

- tectum. *PLoS One*, 8(9), e73663. <https://doi.org/10.1371/journal.pone.0073663>
- Tong, S. K., Mouriec, K., Kuo, M. W., Pellegrini, E., Gueguen, M. M., Brion, F., ... Chung, B. C. (2009). A *cyp19a1b*-GFP (aromatase B) transgenic zebrafish line that expresses GFP in radial glial cells. *Genesis*, 47(2), 67–73. <https://doi.org/10.1002/dvg.20459>
- Trainor, B. C., Finy, M. S., & Nelson, R. J. (2008). Rapid effects of estradiol on male aggression depend on photoperiod in reproductively non-responsive mice. *Hormones and Behavior*, 53(1), 192–199. <https://doi.org/10.1016/j.yhbeh.2007.09.016>
- Ubuka, T., & Tsutsui, K. (2014). Review: Neuroestrogen regulation of socio-sexual behavior of males. *Frontiers in Neuroscience*, 8, 323. <https://doi.org/10.3389/fnins.2014.00323>
- Vajaria, R., & Vasudevan, N. (2018). Is the membrane estrogen receptor, GPER1, a promiscuous receptor that modulates nuclear estrogen receptor-mediated functions in the brain? *Hormones and Behavior*, 104, 165–172. <https://doi.org/10.1016/j.yhbeh.2018.06.012>
- Wakamatsu, Y., & Weston, J. A. (1997). Sequential expression and role of Hu RNA-binding proteins during neurogenesis. *Development*, 124(17), 3449–3460.
- Wullimann, M. F., & Mueller, T. (2004). Teleostean and mammalian fore-brains contrasted: Evidence from genes to behavior. *The Journal of Comparative Neurology*, 475(2), 143–162.
- Wullimann, M. F., Rupp, B., & Reichert, H. (1996). *Neuroanatomy of the zebrafish brain: A topological atlas*. Basel, Switzerland: Birkhauser Verlag.
- Yamamoto, K., & Vernier, P. (2011). The evolution of dopamine systems in chordates. *Frontiers in Neuroanatomy*, 5, 21. <https://doi.org/10.3389/fnana.2011.00021>
- Zhao, S., & Fernald, R. D. (2005). Comprehensive algorithm for quantitative real-time polymerase chain reaction. *Journal of Computational Biology*, 12(8), 1047–1064.
- Zupanc, G. K. (2008). Adult neurogenesis and neuronal regeneration in the brain of teleost fish. *Journal of Physiology (Paris)*, 102(4–6), 357–373. <https://doi.org/10.1016/j.jphysparis.2008.10.007>

How to cite this article: Maruska KP, Butler JM, Anselmo C, Tandukar G. Distribution of aromatase in the brain of the African cichlid fish *Astatotilapia burtoni*: Aromatase expression, but not estrogen receptors, varies with female reproductive-state. *J Comp Neurol*. 2020;1–24. <https://doi.org/10.1002/cne.24908>